Portland State University

PDXScholar

Dissertations and Theses

Dissertations and Theses

Winter 2-22-2013

Microbial Biomineralization of Iron

Wen Fang
Portland State University

Follow this and additional works at: https://pdxscholar.library.pdx.edu/open_access_etds

 Part of the Biology Commons, and the Cell and Developmental Biology Commons

Let us know how access to this document benefits you.

Recommended Citation
Fang, Wen, "Microbial Biomineralization of Iron" (2013). *Dissertations and Theses.* Paper 664.
https://doi.org/10.15760/etd.664

This Thesis is brought to you for free and open access. It has been accepted for inclusion in Dissertations and Theses by an authorized administrator of PDXScholar. Please contact us if we can make this document more accessible: pdxscholar@pdx.edu.

Microbial Biomineralization of Iron

by

Wen Fang

A thesis submitted in partial fulfillment of the
requirements for the degree of

Master of Science
in
Biology

Thesis Committee:
Todd Rosenstiel, Chair
Radu Popa
Pamela Yeh
Martin Fisk

Portland State University
2013

Abstract

Iron is a common cation in biomineral sand; it is present for example in magnetite produced by magnetotactic bacteria and in iron sulfides produced by sulfate reducing microorganisms. The work presented in this thesis focused on two types of microorganisms capable of forming iron biominerals. In the first project I have studied the effect of O_2 on the respiratory physiology and the formation of magnetosomes by *Magnetospirillum magneticum* AMB-1. In the second project I have studied the relationship between olivine and the activity of dissimilatory sulfate reducing (DSR) microorganisms. For the first project, I grew cells of AMB-1 in cultures with various concentrations of O_2 and monitored growth and the formation of magnetic mineral particles (MMP). Results have shown that AMB-1 cells grew better at 100–225 $\mu MO_2(aq)$ than at lower [O_2], yet the formation of MMP was repressed at ~45 μM $O_2(aq)$ and strongly inhibited at ≥100 μM $O_2(aq)$.These results have helped better understand the dissimilarity between the optimal growth conditions of magnetotactic bacteria and the conditions needed for the formation of MMPs. My results have also shown that the reaction between H_2S produced by DSRs and olivine is abiotic, not catalyzed and exergonic. The pH did not vary significantly during this reaction and pH variation (in the 5-9 range) did not significantly influence this chemical reaction. Bicarbonate inhibited the reaction between H_2S and olivine, but not the chemical equilibrium. Phosphate, a weak iron chelator, influenced the equilibrium of the reaction and it is assumed to help increase the rate of olivine weathering in the presence of DSRs. The activity of DSRs was positively influenced by the presence and abundance of

olivine. Based on my results I propose that olivine help DSR obtain energy more efficiently, but does not represent a source of energy or nutrients for the cells. These results helped better understand the formation of iron biominerals and signatures of this activity.

Dedication

I would like to dedicate this work to my loving parents:
Weicheng Fang and *Yunxian Li*.

Table of Contents

List of Tables

List of Figures

Glossary of Scientific Abbreviations

AO	Acridine orange stain
APS	Adenosine phosphosulfate
BCM	Biologically controlled mineralization
BIM	Biologically induced mineralization
CRB	Columbia River basalt
DSR	Dissimilatory sulfate reducing
DSRs	Dissimilatory sulfate reducers
FGD	Flue-gas desulphurization
LASP	Lactate, Acetate, Succinate and Pyruvate
LB	Luria broth
MB	Magnetotactic bacteria
MMP	Magnetic mineral particles
PM	Paramagnetic
RML	Relative magnetite load
SD	Standard deviation
SP	Solubility product
SPM	Superparamagnetic
TEM	Transmission electron microscopy
XRD	X-ray diffractometry

Chapter 1
Introduction

Biomineralization processes, where organisms form inorganic minerals, are a widespread phenomenon. They occur in almost all major taxonomic groups to be able to form mineral, and over 60 different minerals made with the help of organisms have been yet identified (Sigel et al., 2008; Lowenstan and Weiner, 1989; Simkiss and Wilbur, 1989). The first book about biomineralization was published in 1924 by Schmidt W.J., since then the subject has continued to intrigue a dedicated community of scientists (Weiner and Dove, 2003). Until the early 1980s the field was known as "calcification", reflecting the predominance of biologically formed calcium-containing minerals (Weiner and Dove, 2003). After that, more and more biogenic minerals were discovered that contained other cations such as Mg, Fe, Zn, Sr and Ba, and the field became known as "biomineralization". Actually, the term biomineral refers not only to a pure mineral produced by living organisms, but also to products that are containing both mineral and organic components.

Calcium-bearing minerals comprise about 50% of all known biominerals (Lowenstam and Weiner, 1989). Because calcium fulfills many fundamental functions in the cellular metabolism (Simkiss and Wilbur, 1989), widespread usage of the term calcification still exists. Iron containing biominerals are also known to be associated with many organisms. This is probably due to the important role played by iron in many metabolic processes, the toxicity of ferrous iron products and the easy oxidization of iron with O_2 into insoluble ferric iron products at neutral pH (Frankel, 1990). Iron

biominerals also influence properties such as hardness, density and magnetism (Frankel, 1990).

One important iron biomineral is the iron oxide magnetite, Fe_3O_4, which has a cubic, inverse spinel structure. Uniformly-sized particles of magnetite, arranged in chains, are found in magnetotactic bacteria (Blakemore, 1975; Kirschvink, 1980; Bazylinski and Frankel, 2004). These particles are often enclosed in membrane vesicles. Structures consisting of a magnetic particle and its enveloping membrane are known as magnetosomes (Blakemore, 1975). Magnetite is also found in the radular teeth of chitons (marine mollusks from the class *Polyplacophora*) (Lowenstam, 1962) and other organisms as diverse as honeybees and salmon (Kirschvink et al., 1985). Because of their magnetosomes, magnetic bacteria passively orient and then actively migrate along the local magnetic lines, which in natural environments are defined by the geomagnetic field (Frankel et al., 1998). The function of magnetite in chitons is probably related to its hardness, but its function in organisms other than magnetotactic bacteria and chitons is still unknown. Possibly they are related to sensing the direction or magnitude of the geomagnetic field (Frankel, 1990).

Another class of iron biominerals is represented by iron sulfides, often a byproduct of sulfate reduction by bacteria and archea in sediments. Crystalline structures such as pyrites (FeS_2) are known for many years (Trudinger et al., 1972). Jones et al. at 1976 reported intracellular, amorphous iron sulfides in some sulfate reducing bacteria. Also, crystalline particles of greigite (Fe_3S_4) and pyrite have been reported in magnetotactic bacteria from marine sulfidic environments (Bazylinski et al., 1988).

Lowenstam et al. at 1981 have distinguished between biologically induced mineralization (BIM) and biologically controlled mineralization (BCM). In BIM , cellular export of metabolic products results in extracellular mineral formation with ions present in the environment (Frankel, 1990). In this situation, cell surfaces often act as causative agents for nucleation and subsequent mineral growth (Weiner and Dove, 2003). The biological system has little control over the type and habit of biominerals forms., However, the metabolic processes employed by organism influence chemistry via changes in pH, pCO_2 and various secretion products (McConnaughey, 1989; Fortin et al., 1997). In BCM, the mineral phases are deposited in or on preformed organic vesicles or matrices produced by the organism (Frankel, 1990). That means the organism uses cellular activities to direct the nucleation, growth, morphology and final location of the mineral (Weiner and Dove, 2003). Thus, the BIM processes are not controlled by the organism and the mineral particles typically have a large size distribution and no unique morphology, while BCM processes involve highly controlled mineralization and the particles often have a narrow size distribution.

Magnetite (Fe_3O_4) formation occurs by both BIM and BCM, it is done by dissimilatory iron-reducing bacteria and magnetotactic bacteria, respectively. The formation of iron sulfides also occurs by both BIM and BCM, during the activity of sulfate-reducing bacteria and magnetotactic bacteria.

General approach

This thesis includes results of studying two classes of iron biominerals (magnetite formed by BCM and iron sulfides formed by BIM) and two types of microorganisms (magnetotactic bacteria and dissimilatory sulfate reducing bacteria).

1. The first project focuses on the effect of O_2 on the respiratory physiology and magnetosome formation in *Magnetospirillum magneticum* AMB-1. Isolated clones of AMB-1 were grown in liquid cultures with various O_2 concentrations in the gas phase, and we have monitored cell growth, respiration and the formation of magnetic mineral particles (MMP).
2. The second project focuses on the formation of iron sulfides due to the interaction between dissimilatory sulfate reducing microbial communities and olivine surfaces. For this project we have studied the equilibrium and rate of the chemical reaction between hydrogen sulfide and olivine, as well as the effect bicarbonate, phosphate and pH have on this reaction. I have also studied the effect of olivine on the growth rate of dissimilatory sulfate reducing (DSR) communities and isolated and identified microbial species present in this community.

General hypotheses

Hyp1.O_2 excess will inhibit MMP expression in *M. magneticum* AMB-1.

*Hyp2.*In *M. magneticum* AMB-1, the optimal O_2 concentration for the formation of MMPs is similar with the optimum O_2concentration for cell growth.

Hyp3. The reaction between H_2S produced by DSRs and olivine is abiotic and not catalyzed under abiotic conditions.

Hyp4. The growth of DSRs will be positively influenced by the presence of olivine.

Hyp5. The formation of irons sulfides by DSRs in the presence of olivine is an example of BIM.

Chapter 2

Effect of oxidative stress on the growth of magnetic particles in *Magnetospirillum magneticum*

Radu Popa,[1*] Wen Fang,[1] Kenneth H. Nealson,[2] Virginia Souza-Egipsy,[3]

Thelma S. Berquó,[4] Subir K. Banerjee,[4] Lee R. Penn[4]

1 Portland State University, Portland, Oregon, USA.

2 University of Southern California, Los Angeles, California, USA.

3 Center for Astrobiology, Torrejón de Ardoz, Madrid. Spain.

4 University of Minnesota, Minneapolis, Minnesota, USA

International Microbiology, Vol 12, No 1 (2009)

Abstract

Individual magnetosome-containing magnetic mineral particles (MMP) from magnetotactic bacteria grow rapidly such that only a small fraction (<5%) of all magnetosomes contain dwarf (≤20 nm) MMP. Studies of the developmental stages in the growth of MMP are difficult due to the absence of techniques to separate dwarf from mature particles, because the former are sensitive to extraction procedures. Here, O_2 stress was used to inhibit MMP expression in *Magnetospirillum magneticum* strain AMB-1. In addition, defined growth conditions not requiring chemical monitoring or manipulation of the gas composition during growth resulted in the production of cells containing high numbers of dwarf MMP. Cells exposed to different incubation treatments and cells with dwarf MMP were compared to cells with normal MMP with respect to growth, respiration, iron content, and relative magnetite load (RML). The cells were examined by electron microscopy, low temperature magnetometry, X-ray diffraction (XRD), and Mössbauer spectroscopy. In the 0–110 μM O_2(aq) range, growth was positively correlated with [O_2] and negatively correlated with RML. Most MMP formed during exponential growth of the cells. At 50–100 μM O_2(aq) with stirring (150 rpm) and <30% O_2 loss during incubation, MMP expression was strongly inhibited whereas MMP nucleation was not. Cells highly enriched (~95%) in dwarf MMP were obtained at the end of the exponential phase in stirred (150 rpm) cultures containing 45 μM O_2(aq). Only one dwarf MMP formed in each MMP vesicle and the chain arrangement was largely preserved. O_2-stress-induced dwarf MMP consisted of non-euhedral spheroids (~25 nm) that were similar in shape and size to immature MMP from

normal cells. They consisted solely of magnetite, with a single domain signature, no superparamagnetic behavior, and magnetic signatures, Fe(II)/Fe(III) ratios, and XRD patterns very similar to those of mature MMP. These results show that O_2 stress in liquid cultures amended with an inorganic redox buffer ($S_2O_3^{2-}/S^0$) can be used to produce abundant dwarf MMP that are good proxies for studying MMP development.

Key words: *Magnetospirillum magneticum* AMB-1 · magnetotactic bacteria · magnetosomes · biomineralization · magnetite· dwarf MMP

Introduction

Magnetosomes are membrane-bound organelles containing magnetic mineral particles (MMP). They are present in magnetotactic bacteria (MB) (Abreu et al., 2006, 2008; Blakemore, 1975, 1982; Frankel et al., 1997; Keim et al., 2005; Spring, 1995) as well as in many eukaryotes (Kirschvink, 1982; Walker et al., 1984). When aligned in chains, magnetosomes increase the magnetic momentum of MB and (coupled with chemotaxis) help cells move more efficiently toward interfaces of redox comfort (Bazylinski et al., 1997; Frankel, 1981; Steinberger et al., 1994). MMP are euhedral single-domain crystals with species- and even strain-specific shapes ranging from cuboidal, parallelepipedal, or elongated pseudoprismatic to anisotropic (Bazylinski et al., 2003; Thomas-Keprta et al., 2001). Most MB have MMP that are made of magnetite. The majority of these species belong to the α-subdivision of Proteobacteria (e.g.,*Magnetospirillum*, *Magnetococcus*, magnetotactic vibrios), but *Desulfovibrio magneticus* belongs to the δ-subdivision of Proteobacteria (Kawaguchi et al., 1995;

Sakaguchi et al., 1996), and *Magnetobacterium bavaricum* to the family Nitrospiraceae (Spring et al., 1993;, Spring et al., 1995). Most of our knowledge on the formation of MMP is derived from cultures of *Magnetospirillum* (Grunberg et al., 2001; Komeili et al., 2004; Matsunaga et al., 2003; Okamura et al., 2001; Scheffel et al., 2006; Schüler,2002). The biomineralization of MMP in MB includes several steps that are probably common to most species, including iron-uptake (Matsunaga et al., 2003; Nakamura et al., 1995; Paoletti et al., 1986; Schüler, 1999; Schüler et al., 1999), Fe(III)-reduction during or after uptake (Frankel et al., 1983; Schüler, 1999; Schüler et al., 1999; Short et al., 1986), formation of lipid membrane-based MMP vesicles (Bazylinski et al., 2003; Komeili et al., 2004; Matsunaga et al., 2003), accumulation of Fe(II) in the MMP vesicles coupled with an increase in the intra-vesicular pH (Matsunaga et al., 2003 and 2004; Schüler et al., 1998), oxidation of a portion of the intravesicular Fe(II) (Frankel et al., 1983; Schüler et al., 1999), initiation of the MMP (Frankel et al., 1983; Schüler et al., 1999), growth of immature MMP to full size (Blakemore et al., 1985; Matsunaga et al., 2003; Schüler et al., 1997), and the organization of magnetosomes in chains (Komeili et al., 2004; Matsunaga et al., 2003 and 2004). Nonetheless, important questions about the formation of MMP remain unanswered.

We are interested in factors that control the growth of immature MMP to full-size MMP. In general, immature MMP are difficult to study because of their low abundance (<5% of the total MMP population) and the fact that they cannot be distinguished by optical microscopy, are sensitive to extraction procedures (dissolution and oxidation), and participate in magnetic aggregation during centrifugation and thus cannot be

quantitatively separated from the overall MMP population. Our approach to the study of MMP is to produce MB cells containing a high abundance of immature (i.e., dwarf) particles.

MMP development is largely controlled by biochemical and molecular mechanisms, but environmental factors can impair development and thus must be monitored in studies of MMP (Grunberg et al., 2001; Heyen et al., 2003; Matsunaga et al., 2003; Schüler et al., 1998). However, daily verification of the O_2 levels and re-adjustment of the gas composition are often impractical. In the present study, the effects of various levels of initial O_2 and liquid:gas ratios were monitored in cultures of *M. magneticum* strain AMB-1. In addition, these cultures were characterized and compared based on differences in cellular growth, respiration, magnetiteabundance, and iron content. The cells were examined by transmission electron microscopy, low temperature magnetometry, Mössbauer spectroscopy, and X-ray diffractometry (XRD).

Materials and methods

Growth in microaerophilic conditions. *Magnetospirillum magneticum* strain AMB-1 ATCC 700264 (Matsunaga et al., 1991) was grown in microaerophilic conditions with O_2 concentrations between 17 and 240 μM O_2(aq) and 1.4 mM NO_3^- as electron acceptors. The culture medium contained: 5 ml Wolfe minerals/l, 5 mM KH_2PO_4, 1.4 mM $NaNO_3$, 850 μM acetate, 200 mM ascorbate, 1.4 mM succinate, 2.47 mM tartrate, 315 μM sulfur as a $S_2O_3^{2-}$:S^0 mixture (at a ratio of 9:1, used as a reducing agent), 5 ml Wolfe vitamins mix/l, 1.25 mg lipoic acid/l, and 10 ml ferric quinate solution (16.7 mM Fe^{3+}; 10.4 mM

quinic acid)/l. All reagents were purchased from Sigma. Colloidal sulfur (S^0) was obtained by acid disproportionation of $Na_2S_2O_3$. The pH of the medium was adjusted to 7. The medium was distributed in serum bottles and Hungate tubes, which were sealed with 1-cm-thick rubber stoppers and crimped, and the gas phase replaced with different O_2:N_2 gas mixtures. The Wolfe vitamins mix, lipoic acid, and iron quinate were autoclaved, filtersterilized, and then added to the medium. O_2 and N_2 concentrations in the gas phase [O_2(g) and N_2(g)] were monitored by gas chromatography (SRI 310C instrument with a molecular sieve column and TCD detector), and gas pressure was measured with an Omega pressure meter (Omega Engineering). The concentration of O_2 in liquid [O_2(aq)] in the stirred cultures was determined from a saturation of 236 μM O_2 in freshwater with air at 760 mmHg and a temperature of 30°C. The amount of O_2 in the incubation tubes was determined after corrections for changes in pressure and verified based on changes in the N_2:O_2 ratio. After injection of 1.67% O_2(g) in the gas phase, the O_2(g) concentration decreased to ~1.4–1.5% [~16.7 μM O_2(aq)] ~24 h after the nutrients had been autoclaved, due to chemical oxidation of secondary sulfides ($S_2O_3^{2-}+S^0 = H_2S_x$; $2S_xH^- + ½\ O_2 = S^0 + H_2O$). For rapid initiation of the exponential growth phase (~24 h), 6–10 ml medium were inoculated with ~106–107 cells from liquid cultures of exponentially growing *M.magneticum* strain AMB-1 and incubated at 30°C.

Monitorition of cell growth. Cell growth was monitored as the change in A_{420} (using a HP 8452 diode array spectrophotometer); cell density (in cells/ml) was estimated from a calibration of A_{420} against direct cell counts as determined by optical microscopy. Total protein content was determined by the Lowry method (Lowry et al., 1951), and total iron

content by the phenantroline method with hydroxylamine reduction (Greenberg et al., 1985) after acid extraction of the cell pellets with 5 M HCl. The magnitude of the magnetic field (*Bo*) was measured with a triaxial fluxgate magnetometer with a Hall probe (FGM-5DTAA, Walker Scientific) in the 10–8–10–5 T range, and with a gaussmeter (Walker Scientific) in the 10–5–10–3 T range. MMP expression was monitored according to the relative magnetite load (RML), which was derived from changes in light scattering, according to *Bo* of ~4 × 10–3 T, along the light path during spectrophotometric measurements.

$$RML = (B–A)/A \quad (1)$$

where: $A = A_{420}$ without applied *Bo* and $B = A_{420}$ with applied *Bo*.

In our opinion, RML is a better quantifier of MMP expression than the direct difference B–A (Eq. 1) (Schüler et al., 1995), because RML includes a correction for cell density. The two methods were compared in the analysis of cumulative data from 4 days of readings of 21 tubes. The results showed that in the 17–80 μM O_2(aq) range there was better correlation between [O_2(aq)] and RML ($R^2 = 0.7074$, n = 54) than between [O_2(aq)] and (B–A) ($R^2 = 0.093$,n = 54).

Transmission electron microscopy (TEM). Cells were fixed in 2.5% glutaraldehyde, post-fixed in 1% OsO_4, and stained with saturated uranyl acetate in 70% EtOH. Samples were subsequently dehydrated in an EtOH series and embedded in LR-White resin (London Resin, England). A Sorval Porter-Blum MT2-B ultramicrotome was used to cut ~75-nm thin sections, which were mounted on carbon-coated copper grids. TEM images were obtained on an Akashi EM-002B microscope at 100 keV.

Magnetic and XRD measurements. Exponentially growing cells were harvested by centrifugation under 100% N_2. Magnetic measurements included $FC_{(2.5T)}/ZFC_{(2.5T)}$ remanent magnetization curves, hysteresis loops, and ZFC/FC induced magnetization curves, and were carried out with a MPMS-XL SQUID magnetometer (Quantum Design). $FC_{(2.5T)}/ZFC_{(2.5T)}$ remanent magnetization curves [40] were obtained by cooling the samples from 300 to 5 K in a 2.5-T field ($FC_{2.5T}$) and then measuring magnetization, as the temperature was increased stepwise, in a zero field. Then, the samples were again cooled from 300 to 5 K, but in a zero field, subjected to low-temperature isothermal remanence in a 2.5-T field ($ZFC_{2.5T}$), and magnetization was measured during warming of the samples in a zero field. The $FC_{(2.5T)}/ZFC_{(2.5T)}$ remanence curves allowed whole cells, MMP, and synthetic magnetite to be distinguished based on the parameter δ, which is a measure of the remanence lost by warming magnetite particles through the Verwey transition (T_V) at 120 K (Moskowitz et al., 1993; Moskowitz et al., 1988).

$$\delta = [M_{irm}(80) - M_{irm}(150)]/M_{irm}(80) \quad (2)$$

where M_{irm} is the initial saturation of isothermal remanent magnetization (SIRM) remaining at 80 and 150K for $FC_{(2.5T)}$ and $ZFC_{(2.5T)}$ curves (Moskowitz et al., 1993).

The δ_{FC}/δ_{ZFC} ratio is diagnostic of magnetite magnetosomes. For intact chains of unoxidized magnetite magnetosomes, the δ_{FC}/δ_{ZFC} ratio is >2 (Moskowitz et al., 1993), for maghemite samples, the d ratio is close to one, but in this case δz_{FC} and δ_{FC} have values of about 0.05–0.06, while the δ_{FC} values for magnetite magnetosomes are larger (~0.08–0.3). Hysteresis loops, or measurements of magnetization (M) as a function of applied field (H), were obtained by applying fields up to 5 T at 300 K. To investigate the

presence of superparamagnetic (SPM) behavior, ZFC/FC induced magnetization curves were obtained as follows: the samples were cooled in a zero field from a high temperature (in which all particles show SPM behavior) to a low temperature after which magnetization was measured, as the temperature was increased stepwise from 2 to 300 K (ZFC process), in a small applied field (Bo = 5 mT). The sample was again cooled in the same small field and FC magnetization curves were obtained by measuring magnetization of the samples in the field during a stepwise increase in temperature. Several distinct features of superparamagnetism can be verified from these ZFC/FC measurements, such as the blocking temperature (TB) peak of the ZFC magnetization curve. Mössbauer spectra were acquired at room temperature and a conventional constant-acceleration spectrometer (Wissel) was used in transmission geometry with a ^{57}Co/Rh source, using α-Fe at room temperature to calibrate isomer shifts and velocity scale. Fitting was obtained by considering a distribution of quadrupole splitting values.

Results

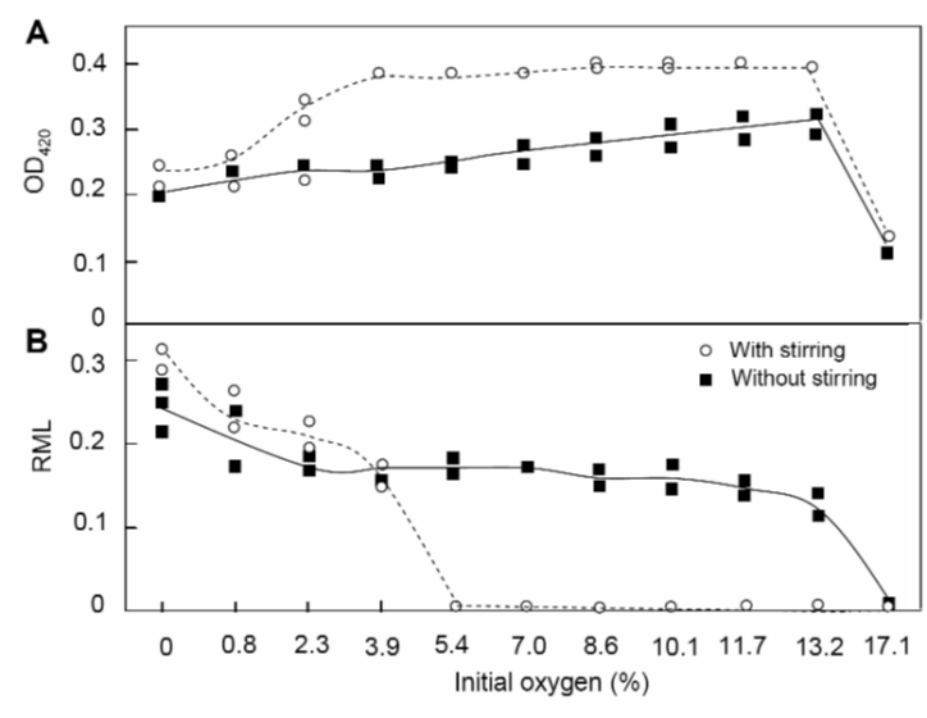

Fig 2.1. The effect O_2 on growth (A) and relative magnetite load (RML) (B) in liquid cultures of *Magnetospirillum magneticum* strain AMB-1 with/without stirring (150 rpm). The initial O_2 values are concentrations in the gas phase at 1 bar.

In many applications involving MB, it is impractical to monitor and correct the O_2(g) concentration daily. It would therefore be very useful to determine specific initial culture and incubation conditions that result in cells with a high abundance of arrested growth magnetosomes after a specific time interval or growth stage, without the need for further manipulation. One approach to this problem is to determine the different initial concentrations of O_2(g) and to stir the cultures to avoid the formation of redox gradients in the liquid column. Accordingly, we verified growth and changes in RML at different initial O_2(g) in stirred (150 rpm) vs. unstirred (27 ml Hungate tubes with 10 ml liquid at

~1 bar) cultures. In the 0–147 μM initial O_2(aq) range, stirring the cultures at high O_2 resulted in faster exponential growth of the cells and larger cell densities in the stationary phase (up to ~5 × 108 cells/ml, ~0.28 g dry weight/l after 72 h). Growth was inhibited above 13.2 % initial O_2(g) (>147 μM O_2(aq) in the stirred cultures), while magnetite formation was strongly inhibited all stirred tubes with >3.9% initial O_2 (Fig. 1). This inhibition was attributed to oxidative stress because magnetite growth requires a ~2:1 Fe(III):Fe(II) ratio, while chemical iron oxidation is fast and has a high equilibrium constant at neutral pH (Heyen et al., 2003; Matsunaga et al., 1991). TEM analysis of the non-stirred cultures showed a dominance of large magnetosomes irrespective of the initial O_2 concentration, a lower number of MMP per cell at the highest initial O_2(g), and no sizable increase in the abundance of dwarf MMP. In stirred cultures, however, cells incubated in 0.8% initial O_2(g) [~8.9 μM O_2(aq)] formed mostly normal MMP. A high abundance of dwarf MMP and very few mature MMP was obtained at 5.4% initial O_2(g) [~60.3 μM O_2(aq)], and very few, mostly dwarf, MMP were formed by cells incubated at 10.1% initial O_2(g) [~112 μM O_2(aq)]. These results suggested a simple, practical means to obtain arrested growth in MMP without daily monitoring and manipulation of the gas composition, by adjusting the initial gas composition to the correct [O_2] values and by stirring the cultures.

During incubation, the O_2 concentration decreases due to chemical oxidation and respiration, which makes it difficult to identify O_2 conditions optimal for the expression of dwarf MMP. It was therefore necessary to limit depletion of the O_2 pool and to monitor its evolution. This was accomplished using stirred cultures with a larger

gas:liquid ratio (27 ml Hungate tubes with 7 ml of liquid culture) and by increasing the initial gas pressure to 1.2–1.4 bar. Under these conditions the $O_2(g):O_2(aq)$ molar ratio was ~125:1 at 30°C and pH 7. Gas pressure, cell density, RML, $O_2(g)$, and $N_2(g)$ were monitored daily in 21 culture tubes containing AMB-1 at seven initial $O_2(g)$ concentrations in the range 17–225 μM $O_2(aq)$. Controls consisted of 21 tubes treated the same way but without cells. Exponential growth occurred between 24 and48 h in all tubes containing cells. During this 24-h interval, the O_2 concentration did not decrease by more than 25% and the generation time was shorter at higher O_2 concentrations (Fig. 2). The average $O_2(g)$ values between the 24- and 48-h readings for the seven O_2 treatments were 20, 37, 53, 78, 92, 110, and 190 μM. The negative correlation between growth rate and magnetite production in the 20–92 μM $O_2(aq)$ range (Fig. 2B) indicated that that the O_2 conditions optimal for the growth of strain AMB-1 are independent of those optimal for MMP development. The sharpest drop in RML occurred in the 53–78 μM $O_2(aq)$ range.

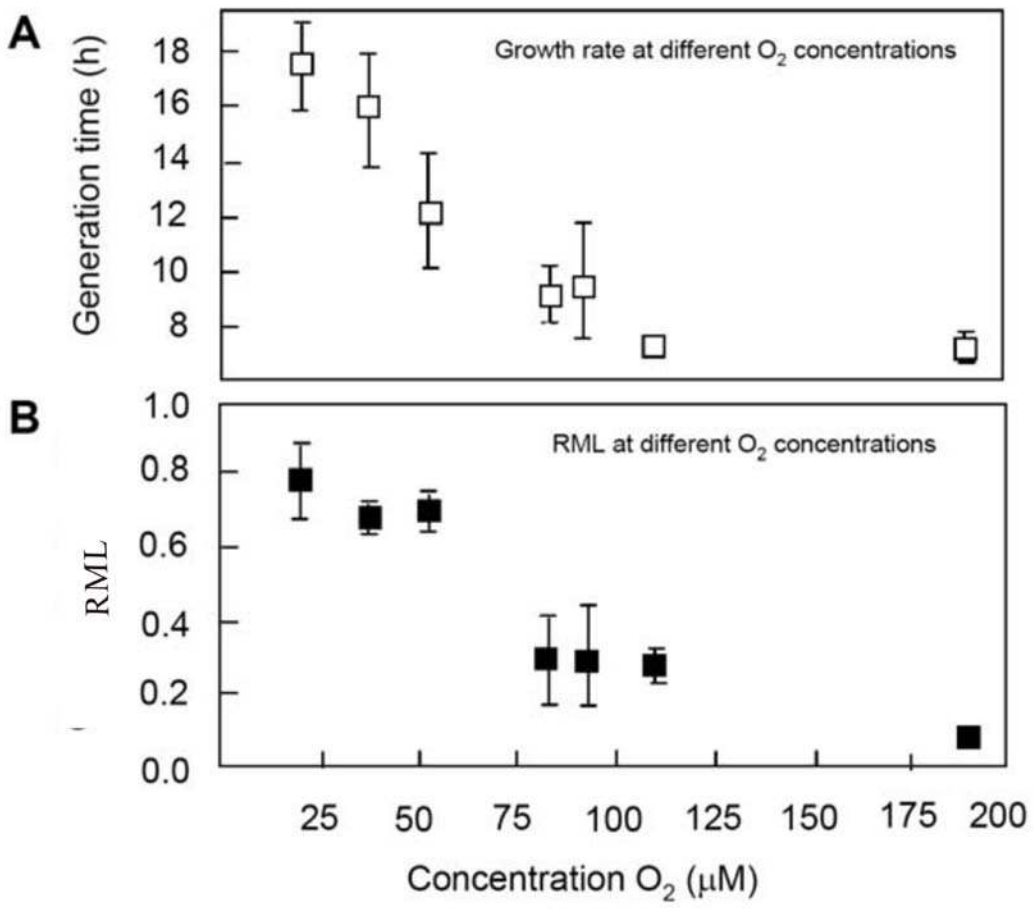

Fig 2.2. (A) The growth rate of *Magnetospirillum magneticum* strain AMB-1, measured during exponential growth at 24-h intervals, increases with [O_2(aq)], reaching a maximum at 110 μM O_2(aq). (B) MMP expression was inhibited at higher [O_2], dropping sharply between 53 and 78 μM O_2(aq). The O_2 concentrations indicated in the graph are averages between triplicate tubes measured after 24 and 48 h of incubation and after corrections were made for changes in pressure. During this 24-h interval the O_2 concentration did not decrease by >20%. Error bars are 1 SD.

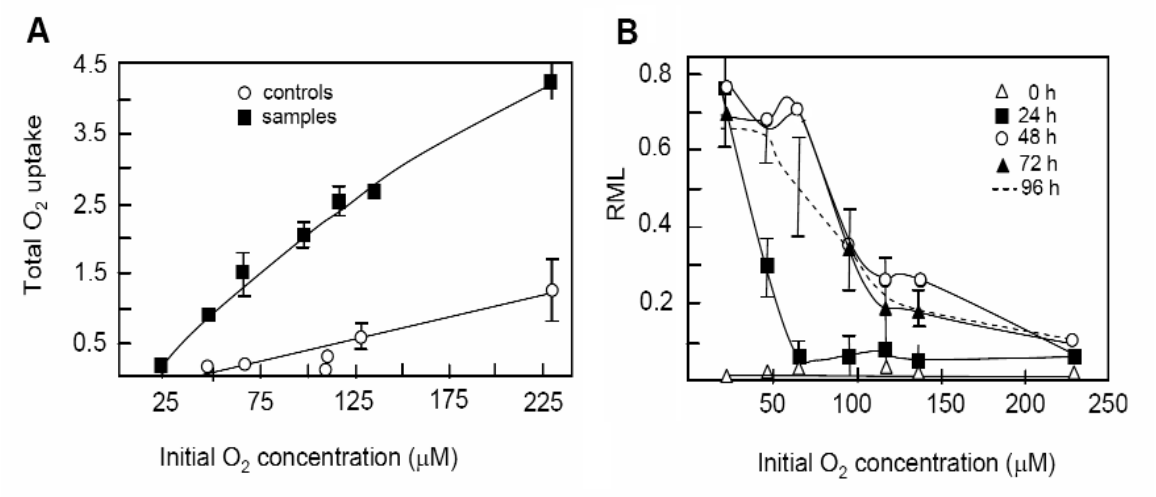

Fig 2.3. (A) Overall O_2 consumption during the incubation of strain AMB-1 cultures, measured after 96 h. The relative contributions of chemical oxidation (controls) and chemical oxidation plus O_2-respiration (samples) are shown. (B) Changes in MMP expression (measured as RML) during incubation with different initial [O_2(aq)] indicate that maximum MMP expression is reached at the end of the exponential phase (48 h in this culture).

After 96 h of incubation, O_2 consumption due to respiration was about four times larger than the effect of chemical oxidation (Fig. 3A). Yet, because respiration is sensitive to changes in [O_2], it is generally recommended to avoid interpreting respiration results when [O_2] changes by ≥ 30% between successive readings. For this reason, and because cells in the lag and stationary phases may express different respiration values, O_2 respiration was calculated only during the 24-h interval that corresponded to exponential growth (24–48 h). To calculate the total O_2 respired by cells of strain AMB-1, corrections were made for changes in pressure and for chemical oxidation, predicted from controls at similar [O_2(aq)]. A positive correlation ($R^2 = 0.7609$; n = 20) was found between the respiration rate and [O_2(aq)], such that μmol O_2 respired × 10^{-10}cells/h = 1.00608 + 0.03299 × [O_2(aq)] (in μM). A comparison of the changes in RML during

growth at different initial O_2 concentrations showed that cells of strain AMB-1 formed magnetosomes mostly during exponential growth (Fig. 3B) and that a subsequent drop to <100 μM O_2(aq) at 72 and 96 h, after cells entered the stationary phase, did not restore the RML (results not shown). The expression of MMP remained low in all cultures in which the initial [O_2(aq)] was >100 μM. It must be emphasized here that these results are dependent on culture stirring; without stirring, cells form large amounts of MMP even at high [O_2(g)].

Magnetic bacteria also store iron in inorganic deposits other than magnetosomes, such as ferritin granules (Bertani et al., 1997) and vacuoles enriched in amorphous iron phosphate (Cox et al., 2002). Although such iron reserves are difficult to quantify, they may play important roles in the ability of the cells to form magnetosomes. In addition, the dynamics of these non-MMP deposits may be controlled by oxidative stress and are thus connected with the growth of MMP. Accordingly, total iron content of *M. magneticum* strain AMB-1 cells was measured in four treatments (18.6 vs. 50 μM O_2(aq), and 0 vs. 150 rpm). To limit changes in [O_2] during incubation, filter-sterilized gas mixtures (O_2 in N_2) containing 1.7 and 4.5% O_2, respectively, were injected every 12 h; the pressure was kept at ~1.3–1.4 bar. Cells were sampled after 48 h (upper exponential phase). The iron content was: 3.8 ± 0.1 mg Fe/mg protein in the 18.6 M O_2(aq)/0 rpm treatment, 2.5 ± 0.2 mg Fe/mg proteins in the 18.6 M O_2(aq)/150 rpm treatment, 5.6±0.5 mg Fe/mg proteins in the 50 mM O_2(aq)/0 rpm treatment, and 1.7±0.2 mg Fe/mg proteins in the 50 μM O_2(aq)/150 rpm treatment. Surprisingly, although RML was larger in the 18.6 μM O_2(aq) treatments, the 50 μM O_2(aq)/0 rpm cultures accumulated the largest

amount of iron. Except for the 50 μM O_2(aq)/150 rpm treatment (which resulted mostly in dwarf MMP), all other treatments led to ~95–100% normal MMP. Since dwarf MMP are only 15% of the size of mature MMP (Fig. 4), a significant part of the iron from cells grown at 50 μM O_2(aq) is probably not stored in magnetosomes. However, given the variability of these measurements, the obstacles to exactly measuring the average number of MMP per cell, and the as-yet unclear relationship between RML and the amount of magnetite made, it was difficult to quantify the intracellular non-MMP iron deposits.

The ultrastructure and arrangement of MMP resulting from the different treatments were analyzed by TEM (Fig. 4). The cells were incubated for 4 days at 30°C in 140-ml serum bottles with 50 ml of liquid medium. In the O_2-stress treatments, premixed gas was injected daily to maintain a concentration of 4% in the gas phase (~45 μM). Under 0% O_2 (0 rpm, or 150 rpm) and 4% initial O_2 (at 0 rpm), only normal mature MMP were formed, with no notable differences between treatments. The mature MMP were euhedral, 59 ± 5 nm vs. 42 ± 7 nm in size within the single domain of magnetite. In contrast, MMP formed under O_2 stress (45 μM O_2; 150 rpm), were smaller, non-euhedral spheroids, ~25 ± 4 nm (hence dwarf MMP), with some as small as 10 nm. If dwarf MMP are made solely of magnetite (see below), this size is still within the single domain. A few of these particles (generally <10%) had elongated shapes (1.5:1 length:width ratio) but still were not euhedral. Dwarf MMP were also present in cells with normal MMP, albeit at low abundance (~12–14%). In cells with dwarf MMP, a slightly elevated number (11 2 vs. ~5±2% in cells with normal MMP) of non-aligned MMP were found. The total number of MMP per cell was almost the same between treatments, ranging between 8

and 25 per cell; however, the total number of MMP per cell observed by TEM thin sections has to be taken as an underestimate. Dwarf MMP (≤25 nm) were also found in cells with normal MMP, but they represented ≤5% of the population and were more frequently distributed toward the ends of the chain, suggesting terminal growth of the MMP chain. In cells placed under O_2 stress (45 μM O_2; 150 rpm), the abundance of dwarf MMP was very high (>95%). Without exception, no more than one MMP was ever found per magnetosome vesicle, although a few vesicles (~3–4%) did not contain MMP. In some TEM images, positive identification of some of the vesicles and of the dwarf MMP was difficult. There was no significant difference in the abundance of empty MMP vesicles between the different treatments, indicating that 45 μM O_2(aq) stress did not inhibit nucleation but only MMP growth. The morphology of the few dwarf MMP contained in cells with normal MMP was very similar with the morphology of the dwarf MMP from cells subjected to O_2 stress. Euhedral MMP <20 nm in size were never found, irrespective of the treatment.

To address whether dwarf MMP are similar in composition to normal MMP, cells with normal and dwarf MMP were compared during two different treatments: ~18.7 μM O_2/150 rpm (for normal MMP) and O_2-streesed cultures ~45 μM O_2/150 rpm (for dwarf MMP). The large amounts of samples needed for the magnetic measurements were obtained by culturing the cells in 1- to 2-l serum bottles with 20–25% liquid medium (as shown in Materials and methods). The medium was autoclaved with ~1.67% O_2 in the gas phase and the gas composition adjusted after cooling to the desired [O_2], adjusted the pressure at ~1 bar. One ml of inoculum from a culture of AMB-1 in late exponential

phase was added per liter and the cultures incubated for 72 h at 30°C. After centrifugation, the pellet obtained from cultures with normal MMP was dark-gray to black, uniform, with a thin white upper layer, while pellets of cells with dwarf MMP were heterogeneous. The upper part of the pellet (~90%) was white, while the bottom part was gray with black spots. We assumed that this heterogeneity was due to cells with different abundances of dwarf MMP, or to a small population of normal size magnetosomes still present in the O_2-stressed cultures, or to an agglomeration of MMP as a result of centrifugation and poor chain alignment. TEM analysis of these pellets indicated that dwarf MMP were present, abundant, and similar in both the upper and lower parts of the pellets of O_2-stressed cells, and that the sizes of the MMP did not significantly differ between these subsamples.

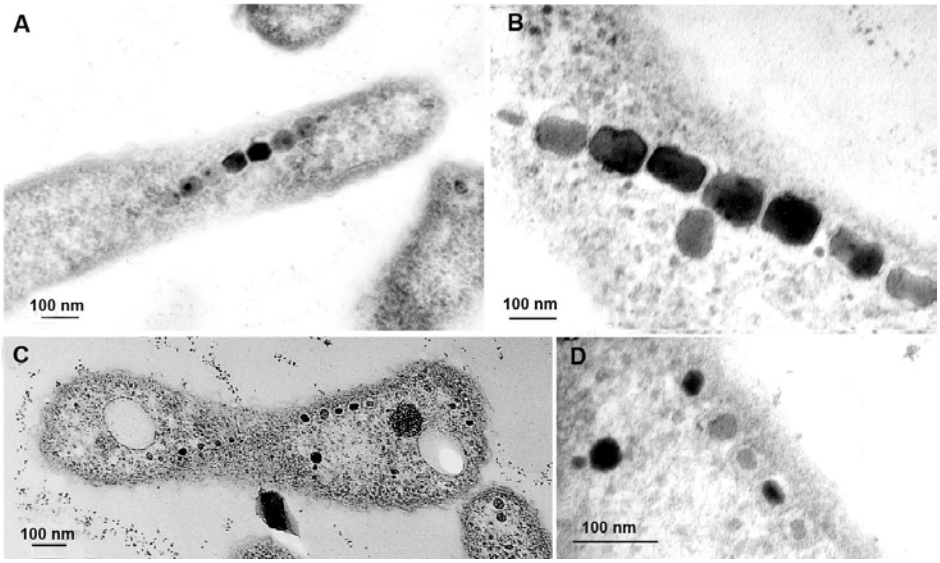

Fig 2.4. Transmission electron micrographs of magnetosomes from cells of *Magnetospirillum magneticum* strain AMB-1. (A) Normal MMP formed under 0% N_2 and 150 rpm. (B) Normal MMP observed at ca. 140,000 × magnifications. (C) Dwarf MMP formed under 4% O_2 and 150 rpm. (D) Dwarf magnetosomes observed at ca. 140,000 × magnifications.

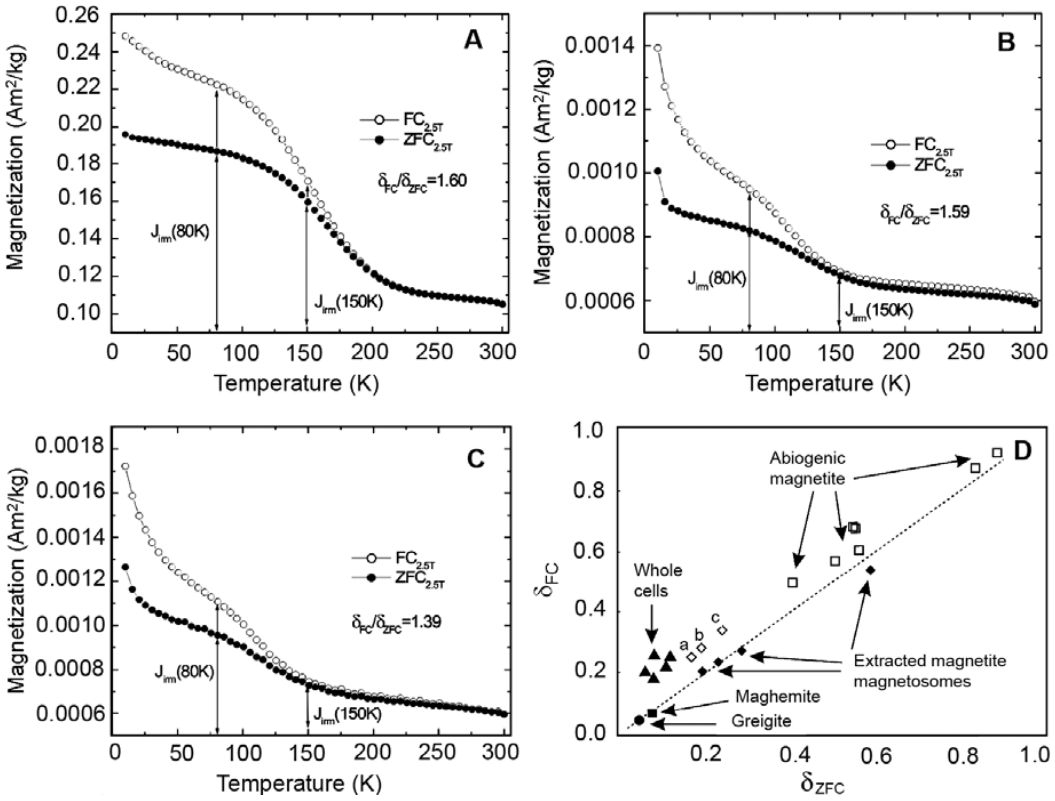

Fig 2.5. $FC_{(2.5T)}/ZFC_{(2.5T)}$ remanent magnetization curves showing Verwey transitions and δ_{FC}/δ_{ZFC} ratios. (A) Pellet of cells with normal MMP. (B)Upper part of the cell pellet containing dwarf MMP. (C) Lower part of the cell pellet containing dwarf MMP. (D) δ_{FC}/δ_{ZFC} plot of the A, B, and C samples relative to data on other published samples (Moskowitz et al., 1993).

We then sought to determine whether different parts of the O_2-stressed cell pellets contained the same type of magnetic materials. Three types of samples were compared: (A) pellets of cells with normal MMP, (B) the upper, white part of the pellets with dwarf MMP, and (C) the lower, dark part of the pellets with dwarf MMP. The $FC_{(2.5T)}/ZFC_{(2.5T)}$ remanent magnetization curves showed very similar patterns between samples B and C, and all samples had Verwey transitions at ~120 K, characteristic for magnetite (Fig. 5). The contribution of paramagnetic (PM) materials was larger in B and C than in normal MMP samples; this was partly expected because cells with dwarf MMP have less Fe and

magnetite than cells with normal MMP. All samples showed a δ_{FC}/δ_{ZFC} behavior between whole cells and extracted magnetosomes; which was also expected since dwarf MMP were not extracted from the cells, in order to limit dissolution, oxidation, and chain breakage. A value of ~1 for δ_{FC}/δ_{ZFC} indicates isolated magnetite particles while a value of ~2 indicates perfectly aligned magnetite chains (Moskowitz et al., 1993). No significant differences in the level of alignment between B (δ_{FC}/δ_{ZFC} = 1.59) and A (δ_{FC}/δ_{ZFC} = 1.60) were found whereas smaller values (δ_{FC}/δ_{ZFC} =1.39), an indication of poorer alignment, were obtained for C. It was previously observed (Moskowitz et al., 1993) that the conversion of magnetite MMP to maghemite (such as during oxidation) reduces δ_{FC} and δ_{ZFC} close to 0.05–0.06 and brings the δ_{FC}/δ_{ZFC} ratio to~1. We found δ_{FC}/δ_{ZFC} ratios <2 and thus inferred no evidence of magnetite alteration.

Samples A, B, and C (Fig. 5) were also compared by hysteresis loop analysis (data not shown). Paramagnetic (PM) and ferrimagnetic contributions in all samples were recorded. In addition, the PM effect was stronger in samples with dwarf MMP, supporting the results presented above (namely, Fe composition and $FC_{(2.5T)}/ZFC_{(2.5T)}$ ratio). The hysteresis parameters at 300 K, the saturation magnetization (M_s), and the saturation remanent magnetization (M_{rs}) were very similar between the A and B samples. Using the known value of M_s for magnetite, we estimated that the dried-pellet samples each contained <1% magnetite. Additional information was obtained from the M_{rs}/M_s ratio, which for whole-cell samples at room temperature is ~0.5 for a random distribution of uniaxial "single domain chains" (Moskowitz et al., 1993). The values obtained for the A and B samples were smaller than expected (~0.4); this may have been due to broken

chains, which is a typical artifact of extended centrifugation. It was difficult to determine a precise M_{rs}/M_s value for the C samples because of their high PM contribution. Mössbauer spectra showed only doublets, which may have indicated PM or SPM iron phases, thus confirming previous reports (Frankel et al., 1985), but ZFC/FC induced magnetization analysis showed only PM and not SPM behavior. Lastly, XRD analysis showed no significant differences between samples and that the only mineral present was magnetite (results not shown), supporting the previous results.

Discussion

It was previously reported that the expression of MMP in *M. magneticum* strain AMB-1 is optimal at 2.35 μM O_2, is partly inhibited at 11.7 μM O_2, and totally inhibited at 23.52 μM O_2. Without subsequent manipulation of the gas composition, we found that *M. magneticum* strain AMB-1 cells are more tolerant to O_2 stress than previously acknowledged, when an inorganic reductant (such as $S_2O_3^{2-}$:S^0 mixture) is added to the medium. During these incubations, O_2 decreased by 6–45% over 96 h. The initial culture conditions described herein allow a high abundance of dwarf MMP to be obtained without the need for chemical monitoring and periodic adjustment of [O_2]. Cells of *M. magneticum* strain AMB-1 grew better at 100–225 μM O_2(aq) in stirred liquid culture than at lower [O_2], yet the formation of MMP was repressed at ~45 μM O_2(aq) and strongly inhibited at ≥100 μm O_2(aq). Under conditions of ~45 μM initial O2 in liquid, 150 rpm, and 30°C, numerous dwarf magnetosomes, representing ≥ 95% of the total MMP population, formed after 48 h of incubation, and the O_2 concentration decreased by

~20%. The higher respiration rate, faster growth, and higher final density at higher [O_2] supports the conclusion that, in strain AMB-1, the oxidative stress of MMP production does not coincide with the oxidative discomfort of the cells. The total number of MMP was similar between cells with normal MMP and cells with dwarf MMP grown at 45 μM initial O_2(aq) and 150 rpm. Only a small fraction of all dwarf MMP were not aligned. Magnetite was the only magnetic material or mineral detected in strain AMB-1. The smallest dwarf magnetosomes were ~10 nm in size and were very seldom euhedral, but rather irregular spheroids. MMP vesicles with more than one MMP particle were not observed, implying that MMP are initiated from a sole nanocrystallite and that novel magnetosome are added mainly terminally in the MMP chain. Despite the fact that very large populations of dwarf MMP were analyzed (~4×10^{11} per sample), there were no signals of SPM behavior; instead, only SD behavior and a PM signal. The magnetic signatures of cells with dwarf MMP was nearly the same as that of cells with normal magnetosomes, i.e., no ferryhydrite, aligned SD magnetite, no SPM behavior, and enrichment in PM iron.

In earlier models, it was hypothesized that MMP are initiated via: (i) SPM nanocrystallites of magnetite growing into mature single domain particles; (ii) early granules of crystalline or amorphous ferryhydrite, later replaced by magnetite (Frankel et al., 1983; Schüler et al., 1999); and (iii) iron-rich organic matrices, later replaced by magnetite (Matsunaga et al., 2003; Vainshtein et al., 1998). The existence of a short-lived SPM magnetite or ferryhydrite phase during MMP growth cannot be excluded, but a method to systematically stop the growth of all magnetosomes in very early SPM stages

has yet to be found. The MMP were not in physical contact with the MMPmembrane, perhaps indicating that the growth of MMP is controlled via solute chemistry rather than surface contact. The initiation of novel MMP was not observed, probably because the period of growth between early nanocrystallites and dwarf MMP is very short. The culturing conditions proposed herein have a greater effect on the growth of MMP from dwarf to mature MMP than on the formation of dwarf MMP, and can be used to study stages in MMP development.

Acknowledgements. This research was supported by grants from NASA (Astrobiology Institute, Planetary Biology Internship), National Science Foundation (NSF), and the University of Southern California Undergraduate Research Program. Special thanks to Dr. S. Lund of the USC for help with calibrating RML readings vs. the abundance of cellular magnetite. This study was also supported by NSF grant EAR 0311869, from the Biogeosciences program, the Institute for Rock Magnetism (IRM), funded by the Earth Science Division of NSF, and the W. M. Keck Foundation and University of Minnesota, IRM publication # 0613.

Chapter 3

Dissimilatory sulfate reduction on olivine surfaces

Abstract

Dissimilatory sulfate reducing (DSR) microorganisms play important roles in the geochemical cycles of sulfur and metals. These microorganisms are anaerobic and are capable of oxidizing organic molecules and H_2 with sulfate, producing reduced sulfur chemicals including hydrogen sulfide (H_2S) which is toxic to the cells. The growth of DSRs in cultures is faster when iron is present which reacts with H_2S and forms iron sulfide precipitates. We found abundant growth of DSRs in the presence of olivine, an iron containing mineral ($(Mg,Fe)_2SiO_4$). In this work we have studied the reaction between H_2S and olivine and the growth of DSRs in the presence of olivine. Our results show that the reaction between H_2S (produced by DSRs) and olivine is abiotic and not catalytic. The growth of DSRs was positively influenced by olivine, though olivine (apart from iron and magnesium) is not a source of nutrients microorganisms.

Introduction

Olivine description and chemistry

Olivine ($(Mg,Fe)_2SiO_4$) is a metal silicate mineral very common on earth. It forms in igneous rocks such as basalt during the cooling of lava and magma. In some cases olivine crystals are also present in sedimentary deposits such as soil, sediments and sand. Olivine only contains iron in reduced form (Fe(II)) and a very thin layer of oxidized iron (Fe(III)) may cover the surface of crystals. The magnesium to iron ratio in

olivine varies. Forsterite olivine contains 0% iron while fayalite olivine contains 100% iron. The designation for olivine is based on the % magnesium. For example, forsterite is labeled Fo_{100}, while fayalite is Fo_0. In our experiments we have used Fo_{90} olivine.

Although the abiotic weathering of olivine was intensely studied, little work exists on its bioweathering (Welch and Banfield, 2002; Wogelius and Walther, 1992; Siever and Woodford, 1979; Popa et al., 2012). This limited work is due to complications resulting from oxidative dissolution reactions and subsequent precipitation of iron oxyhydroxide phases on olivine surfaces (Welch and Banfield, 2002). Past research indicated that the oxidation of Fe-rich silicate minerals may enhance or inhibit their dissolution rate. The extent of this reaction was generally determined based on the net release of materials in solution. White and Yee (1985), while studying the dissolution of several Fe-silicate minerals, found increased dissolution rate under oxidizing conditions leading to Fe^{3+}. In the pH range 1.5 to about 10, this process consumed dissolved oxygen at a rate that increased at lower pH. Wogelius and Walther (1992) and Siever and Woodford (1979) reported decrease in long-term dissolution rate of fayalite, attributed to the precipitation of iron oxyhydroxide phases, coating the olivine surfaces.

Energy rich chemicals (such as methane and hydrogen) can occur in the presence of olivine. For example, serpentinite is formed from olivine and may generate methane (CH_4) and hydrogen (H_2) under anaerobic conditions. The utilization of either H_2 or CH_4 by chemoautotrophic microorganisms may provide the energy required for microbial growth on olivine (Santelli et al, 2001; Welch and Banfield, 2002; Garcia et al., 2005; Longazo et al., 2001; Josef et al., 2007). Organotrophs may also influence olivine

dissolution. For example, Garcia (2005) showed that in the presence of olivine, *Escherichia coli* caused an enrichment of their host solution in ^{24}Mg relative to heavier isotopes. Santelli et al. (2001) and Welch and Banfield (2002) used iron-oxidizing bacteria (*Acidithiobacillus ferrooxidans*) in low-pH cultures to examine changes in both the olivine surface morphology and the chemistry of the culture media. Josef (2007) found that some microorganisms act to suppress dissolution of olivine instead of enhancing dissolution, and also that abiotic dissolution overshadows microbial enhanced dissolution. Longazo et al. (2001) placed unidentified bacillus bacteria, isolated from the Columbia River aquifer, into cultures with olivine and no Fe or Mg and showed that these microorganisms have created weathering features on olivine surfaces.

The relationship between the growth of dissimilatory sulfate reducing (DSR) microorganisms and olivine has never been studied. In theory, the sulfide produced by DSRs should react with iron on olivine surfaces and speed up its dissolution. This study is the first report that connects DSRs with olivine, and is important for understanding olivine bioweathering in DSR communities and the influence of olivine on DSR communities.

Iron sulfide chemistry

Iron sulfides are an essential part of the global biogeochemical cycles of sulfur and iron. Iron sulfides are key indicators for understanding the evolution of earth's subsurface geochemistry and early history. For example, studying the evolution of

atmospheric O_2 can relies (among others) on analyses and interpretations of iron sulfides (particularly pyrite, FeS_2), in ancient sedimentary rocks (Rickard, 2007).

Iron sulfides exist in many forms and compositions (i.e. iron:sulfur ratios) and may be amorphous or crystalline. They also vary in solubility and degree of oxidation (Vaughan and Craig, 1978; Rickard, 2007; Harmandas and Koutsoukos, 1996; Wolthers et al., 2003). Some of the most important iron sulfides are discussed next. Amorphous FeS is a non crystalline precipitate of Fe^{2+} and S^{2-} with a solubility product (SP) of about $10^{-7.5}$. Amorphous FeS is abundant in natural environments and plays an important role in geochemical processes and the fate of contaminants. For example, it is an important diagenetic product in marine sediments (Michel et al., 2005), is environmentally significant in the sequestration and remobilization of heavy metal contaminants (such as Cu, Cd, As, Ni and Co), and has recently been shown to react with contaminants such as dissolved Cr species (Mullet, 2004). Pyrrhotite ($Fe_{1-x}S$) is a mineral with monoclinic crystal structure. It is the most abundant iron sulfide on earth and the solar system, though it is rarely found in marine systems. Troilite (FeS) is a stoichiometric compound with hexagonal symmetry. Mackinawite ($Fe_{1+x}S$), is the least stable iron sulfide mineral, with tetragonal layered crystal structure and it is widespread in low-temperature aqueous environments. Greigite (Fe_3S_4) is a fairly widespread ferromagnetic mineral, more frequently associated with freshwater systems. Unlike all other iron sulfides (which only contain sulfur in S^{2-} form), pyrite and marcasite (FeS_2) contain sulfur in a more oxidized state (S^-). They are also highly insoluble, SP $\approx 10^{-24}$(Rickard, 2007).

In the presence of O_2, mineral iron sulfides are more stable than amorphous FeS. The evidence that amorphous FeS is dominant in a mixture can be obtained by exposure to air for 24-48 hours. Upon oxidation, amorphous FeS turns into rusty iron oxides and elemental sulfur.

$$FeSamorph + O_2 \rightarrow Fe^{3+} + S$$

Though details vary greatly, the general form of the reaction between iron and sulfur is:

$$Fe + HS^- \rightarrow FeSx + H^+$$

First iron sulfide precipitates resulting from this reaction are either amorphous FeS or crystalline mackinawite. Reaction between sulfide and ferrous solutions resulted in poorly crystalline or amorphous precipitates, whereas reactions with metallic iron favored mackinawite (Csákberényi-Malasicsa et al., 2012). This reaction occurs in the absence of oxygen which oxidizes Fe(II) to Fe(III) and sulfide to S^o. In anoxic, yet mildly oxidizing conditions, such as when oxygen is absent but Fe(III) or S^o are present the reaction between Fe(II) and H_2S may lead to pyrite or marcasite (FeS_2).

In strictly anoxic sediments:

$$FeS + H_2S \rightarrow FeS_2 + H_2$$

In salt water sediments:

$$Fe^{2+} + S^o \rightarrow FeS_2$$ (Schulz and Zabel, 2000)

This reaction is important, because pyrite and marcasite are highly insoluble and serve as a sink, removing sulfide and metals from the liquid phase.

The biological sulfur cycle

The sulfur cycle includes the processing of sulfur moving to and from minerals, waterway and living systems. This cycle is important in geology because sulfur is in the top ten list of most abundant elements in earth's crust; it reactions are involved in metal recovery and lead to pollution during metal mining as well as in metal and concrete corrosion. Sulfate (SO_4^{2-}) is the second most abundant anion in the ocean. The sulfur cycle is also important for life because sulfur is an element essential in many proteins, enzymatic cofactors and lipids, and because sulfur chemicals can be used by cells to obtain energy. Sulfur occurs in nature in a variety of oxidation states, the three most important being S^{2-} (in sulfide and reduced organic sulfur), S^{o} (elemental sulfur) and S^{6+} (sulfate) (Tang, 2009). Chemical or biological agents contribute to the transformation of sulfur from one state to another, thus microorganisms play an important role in sulfur transformations. For example, H_2S can be oxidized to sulfur or sulfate by sulfide oxidizers, while sulfate can be reduced by DSRs (Robertson, 2006). Figure 3.1 shows a phylogenetic tree illustrating the widespread distribution of various types of sulfur-metabolizing microorganisms including sulfur/sulfide oxidizers and sulfate/sulfur reducers. Because members of both Archaea and Bacteria can use sulfate as a terminal electron acceptor, some researchers use general terms such as sulfate-reducing prokaryotes or sulfate reducing microorganisms. In this paper, we use the term dissimilatory sulfate reducers (DSRs) to broadly refer to members of both prokaryotic domains.

Sulfur oxidizing bacteria can oxidize inorganic sulfur compounds as electron donors. Sulfur oxidizing bacteria include: anoxygenic phototrophs such as green (*Chlorobium sp.*) and purple (*Chromatiaceae sp*.) sulfur bacteria; colorless sulfur bacteria (such as *Thiospira sp., Acidithiobacillus sp.* and the Archaeal *Thermococcus* sp.). Shown below are some of the most important chemical reactions performed by sulfur and sulfide oxidizing bacteria:

Sulfur oxidizing bacteria:

1. Chemoautotrophic (for example *Thiobacillus thiooxidans*):

   $2S^o + 3O_2 + 2H_2O = 2SO_4^{2-} + 4H^+$

2. Anaerobic photoautotrophic (for example *Chloroherpeton thalassium*):

   $S^o + 2CO_2 + 2H_2O = SO_4^{2-} + 2(CH_2O) + 2H^+$ (Ivanov 1981)

Sulfide oxidizing bacteria (for example *Beggiatoa spp*.):

1. Chemoautotrophic:

   $2H_2S + O_2 = 2S^o + 2H_2O$ or

   $H_2S + 2O_2 = SO_4^{2-} + 2H^+$

2. Photoautotrophic:

   $2H_2S + CO_2 = 2S^o + (CH_2O) + H_2O$ or

   $H_2S + 2CO_2 + 2H_2O = SO_4^{2-} + 2(CH_2O) + 2H^+$ (Ivanov 1981)

With regard to reduction processes, some microorganism can reduce elemental sulfur, others can reduce sulfate. Most common chemical reactions produced by sulfate/sulfur reducing bacteria are show below:

Sulfur respiration of sulfur reducing bacteria:

1. Using organic acids as electron donors (*Desulfuromonas acetoxidans*):

   $CH_3COOH + 2H_2O + 4S^o = 2CO_2 + 4H_2S$

This group of sulfur reducing bacteria can also use ethanol, lactate, pyruvate, propanol as electron donors and can live syntrophically with phototrophic green sulfur bacteria which oxidize H_2S to S^o

2. Using hydrogen as an electron donor (e.g. thermophilic anaerobic archaea such as *Thermoproteus sp.*):

   $H_2 + S^o = H_2S$

Chemoheterotrophic sulfate reducing bacteria (e.g. *Desulfobacter* and *Desulfobulbus*):

1. Using hydrogen as an electron donor

   $4H_2 + SO_4^{2-} = H_2S + 4H_2O$

2. Using organic acids as electron donor

   $4CH_3OH + 3SO_4^{2-} = 4CO_2 + 3H_2S + 8H_2O$

This class of DSRs can also use ethanol, lactate and pyruvate as electron donors.

Based on their metabolism, sulfate/sulfur reducing bacteria can be organized in three groups. a) Sulfate reducers capable of using lactate, pyruvate, many alcohols and fatty acids as electron donors and capable of reducing SO_4 to H_2S (some of which produce acetate). b) Sulfate reducers capable of using fatty acids (especially acetate) and

oxidize substrates completely to CO_2, while converting SO_4 to H_2S (some of these microbes can grow chemoautotrophically using H_2 as the electron donor). And c) Dissimilatory sulfur reducers, capable of reducing elemental sulfur to sulfide, but unable to reduce sulfate; these microorganisms are exclusively anaerobic, can use acetate and ethanol as common electron donors and S^o is the sole electron acceptor.

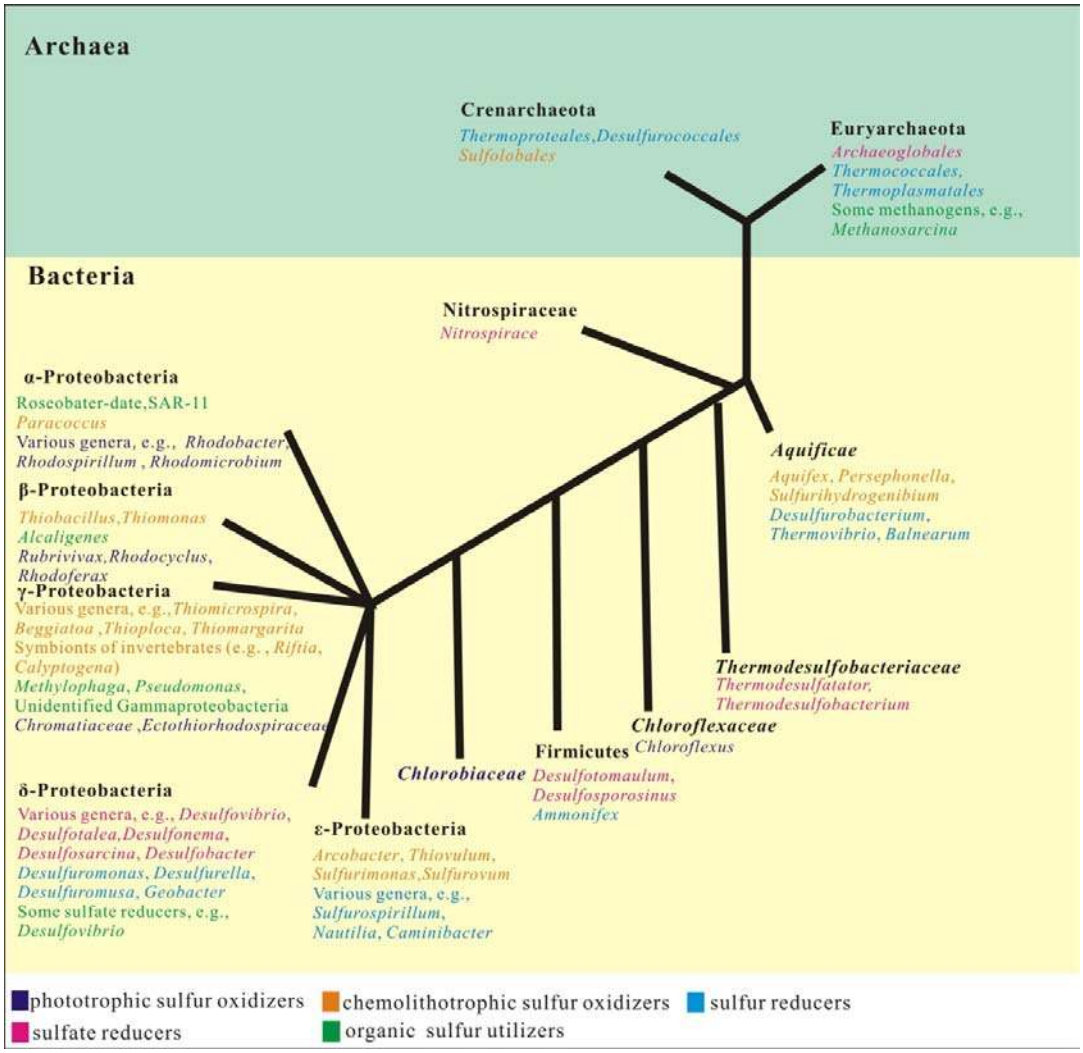

Fig. 3.1. Tree showing the widespread distribution of sulfur-metabolizing microorganisms among major phylogenetic lineages (modified after Stefan, 2007).

Diversity of DSRs

Sulfate reduction may be either an assimilatory process (i.e. assimilatory sulfate reduction), or an example of anaerobic respiration (i.e. dissimilatory sulfate reduction, or DSR) (Fig. 3.2). Assimilatory sulfate reducers convert sulfate into reduced sulfur which they use for constructing organic molecules. DSRs use sulfate as an electron sink and thus as a source of energy. Some sulfate-reducing bacteria also have the capacity to use chemicals such as nitrate and nitrite, ferric iron, other metals, and even oxygen as electron acceptors (Muyzer, 2008). Under low-oxygen or oxygen-free conditions, in environments such as swamps, anoxic sediments, and deep Black Sea water, DSRs oxidize organic matter or hydrogen, and produce hydrogen sulfide. Some of this hydrogen sulfide reacts with metal ions and produce metal sulfides, which appear as black precipitates. DSRs are considered to be some of the oldest types of microorganisms on earth. Isotopic data suggests that DSRs may have existed 3.5 billion years ago, and may have contributed to the sulfur cycle very soon after life first emerged on earth (Barton, 2009). Microbial DSR in anoxic environments is the most important source of low-temperature sulfide in natural waters (Ledin, 1996).

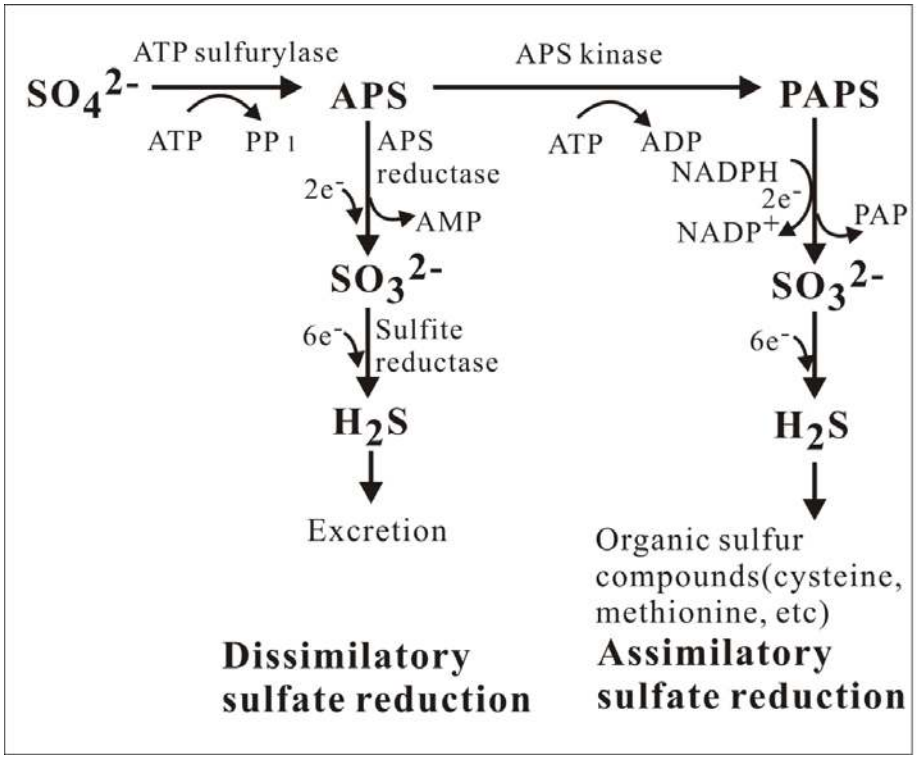

Fig. 3.2. Diagram of differences between assimilatory and dissimilatory sulfate reduction.

Based on comparative analysis of 16S rRNA sequences, DSRs belong with seven phylogenetic lineages, five within the Bacteria and two within the Archaea (Fig. 3.1). Most sulfate reducers are from about 25 genera of the δ-subclass of Proteobacteria, followed by Gram-positive DSR bacteria related to Clostridia (e.g. *Desulfotomaculum*, *Desulfosporosinus* and *Desulfosporomusa*). The third branch is represented by thermophilic sulfate reducers, which includes three lineages, Nitrospirae (*Thermodesulfovibrio*), Thermodesulfobacteria (*Thermodesulfobacterium*) and Thermodesulfobiaceae (*Thermodesulfobium*) (Mori et al., 2003). Within the Archaea,

DSRs are common in the genus *Archaeoglobus* in Euryarchaeota, and *Thermocladium* and *Caldirvirga* in Crenarchaeota (Itoh et al., 1998 and 1999; Rabus, 2006).

Some species of bacteria (important for this study) are facultative heterotrophs and are capable of both dissimilatory sulfate reduction and aerobic or anaerobic organotrophy. Examples include some species of *Pseudomonas aeruginosa* and *Pseudomonas putida* (Thomas C. Montie, 1998; Kliushnikova et al., 1992; Tsakraklides et al., 2002), *Desulfotomaculum nigrificans* (previously *Clostridium nigrificans*) (Campbell and Postgate, 1965).

DSRs can be classified into two groups: complete oxidizers (acetate oxidizers), which have the ability to oxidize the organic compound to carbon dioxide, and incomplete oxidizers (non-acetate oxidizers) which carry out the incomplete oxidation of organic compounds to acetate and CO_2. *Desulfobacter*, *Desulfobacterium*, *Desulfococcus*, *Desulfonema*, *Desulfosarcina*, *Desulfoarculus*, *Desulfoacinum*, *Desulforhabdus*, *Desulfomonile*, *Desulfotomaculum acetoxidans*, *Desulfotomaculum sapomandens* and *Desulfovibrio baarsii* are complete oxidizers (Postgate, 1984; Rabus, 2006). Incomplete oxidizers include *Desulfovibrio*, *Desulfomicrobium*, *Desulfofustis*, *Desulfotomaculum*, *Desulfobotulus*, *Desulfomonile*, *Desulfobacula*, *Archaeoglobus*, *Desulfobulbus*, *Desulforhopalus* and *Thermodesulfobacterium* (Madigan, 2006; Colleran, 1995). The growth kinetics of incomplete oxidizers is generally faster than that of complete oxidizers. Some sulfur reducing bacteria, which is the other group of obligate anaerobes responsible for the production of sulfide, consist of genera such as

Desulfuromonas, *Desulfurella*, *Sulfurospirrilium* and *Campylobacter*. These bacteria can reduce sulfur to sulfide but are unable to reduce sulfate to sulfide (Rabus, 2006).

Mechanism of dissimilatory sulfate reduction (DSR)

DSRs use sulfate as the terminal electron acceptor and organic compounds or H_2 as electron donors. The main steps of DSR oxidation of H_2 are shown next (Fig 3.2):

1. Sulfate, which is fairly stable, is activated by reaction with ATP, forming adenosine phosphosulfate (APS).

   $SO_4^{2-} + ATP \rightarrow APS + PPi$

2. A hydrogenase splits H_2, and the resulting electrons are used to reduce the sulfur atom from APS, releasing sulfite (SO_3^{2-}).

   $APS + H_2 \rightarrow SO_3^{2-} + AMP + H_2O$

   This reaction involves an intermediate electron carrier, cytochrome c3, which is diagnostic for dissimilative sulfate reducers.

3. Using more electrons derived from H_2, sulfite is further reduced to sulfide.

   $SO_3^{2-} + 6\ H^+ + 6e^- \rightarrow H_2S + H_2O + 2OH^-$

Sulfite is reactive and toxic to most organisms and it is generally reduced as soon as it is produced. Bacteria do not wait until all sulfate is exhausted before beginning to reduce the sulfite. The final product, hydrogen sulfide, is also toxic, but as a gas part of it is released in the atmosphere. During these reactions, the hydroxide ion is generated raising the pH.

Distribution of DSRs in the environment

DSRs can be found in many natural and artificial environments where sulfate is present. They have been detected or isolated from mud volcanoes sites in the bottom of the Black Sea (Stadnitskaia et al., 2005), marine sediments (Mussmann et al., 2005, Webster et al., 2006), hydrothermal vents at Guaymas Basin (Jeanthon, 2002), hydrocarbon seeps at Cascadia Margin, Oregon (Knittel et al., 2003), and are also abundant in hypersaline microbial mats (Minz et al., 1999, Rissati et al., 1994).

DSRs have also been detected in extreme environments, for example in extreme pH habitats, in acid mine drainage sites at pH as low as 2 (Sen, 2001) or in alkaline lakes at pH 10 (Geets et al., 2006). DSRs have also been detected and isolated from freshwater sediments (Sass et al., 1998), oil fields (Nilsen et al., 1996), anaerobic waste-water treatment industry (Elferink et al., 1994; Ben-Dov et al., 2007), and even in the rhizosphere of plants (Hines et al.,1999; Bahr et al., 2005).

Most DSRs are free-living, but some are present in syntrophy with other microorganisms. For example, DSRs can grow together with sulfur oxidizing γ – proteobacteria, as endosymbionts in the marine oligochaete worm *Olavius algarvensis* (Dubilier et al., 2001; Woyke et al., 2006). In freshwater environments or water-logged soil with low concentration of sulfate, many species of *Desulfovibrio* and *Desulfomicrobium* have been found capable of growing by fermenting pyruvate to acetate, carbon dioxide and H_2. *Desulfotomaculum* (a Gram-positive, obligately anaerobic), causes the "sulfide stinker", a type of spoilage of canned foods. *Desulfomonas* is an anaerobic DSR, isolated from human feces and thoracoabdominal

areas. *Archaeoglobus* is a thermophilic Archea growing at high temperatures between 60 and 95°C (Klenk et al., 1997).

Biotechnological application of DSRs

Mine waters and industrial effluents may contain high sulfate and metal concentrations and pose significant disposal problems that require urgent solution to avoid serious environmental contamination (Jong and Parry, 2003). In mine waters, sulfate, metalloids (arsenic) and heavy metals (such as copper, nickel, zinc and iron) originate from the chemical or biological oxidation of exposed sulfide minerals. This process also generates acidity (in the form of H_2SO_4) which can also dissolve other minerals, releasing cations (Chang et al., 2000). Thus, there is an increasing interest in the potential biotechnological applications of DSRs as an alternative method for sulfate and heavy metal removal from contaminated sites (Chang et al., 2000; Elliott et al., 1998; Kim et al., 1999). Metal sulfates (of copper, nickel, zinc and iron) are highly soluble, but their corresponding sulfides have low solubility. Thus, under anaerobic conditions, DSRs can be used to sulfate to sulfide, which can react with dissolved metals to form metal sulfide precipitates (Kim et al., 1999). This concept has been applied to immobilize metals from surface water and process water from mining industries (Muyzer et al., 2008).

Another biotechnological application of DSRs is in the removal and reuse of sulfur compounds from waste water (Muyzer et al., 2008). Sulfide is relatively easy to

oxidize. When oxygen is limited, sulfide oxidizing bacteria produce mainly elemental sulfur instead of sulfate.

$HS^- + 0.5O_2 \rightarrow S° + OH^-$

This feature can be used to remove hydrogen sulfide from natural gas or biogas (Janssen et al., 2001). If this is combined with an anaerobic step, it can also be used to treat water and gas containing oxidized sulfur compounds. Firstly, the oxidized sulfur compounds are reduced to sulfide with the help of DSRs. Then sulfide is partially oxidized to S^o. One related application is the flue-gas desulphurization (FGD) technology. Lime or limestone-based wet scrubbing is a commonly applied FGD technology. But, biotechnological FGD (Bio-FGD) was proposed as an alternative based on the following transformations (Muyzer et al., 2008).

1. SO_2 is scrubbed from the flue gas with an alkaline solution to form sulfite

   $SO_2 + OH^- \rightarrow HSO_3^-$

2. Oxygen in the flue gas causes the oxidation of part of sulfite to sulfate

   $HSO_3^- + 0.5O_2 \rightarrow SO_4^{2-} + H^+$

3. In an anaerobic bioreactor, sulfite and sulfate are reduced by DRSs to sulfide

   $HSO_3^- + 6[H] \rightarrow HS^- + 3H_2O$ or

   $SO_4^{2-} + 8[H] \rightarrow HS^- + 3H_2O + OH^-$

4. In a microaerobic reactor, sulfide is oxidized to S^o by autotrophic sulfide-oxidizing bacteria

   $HS^- + 0.5\ O_2 \rightarrow S° \downarrow + OH^-$

In the last step sulfide oxidation, alkalinity is produced, which can be led back to entrap sulfur dioxide on step one. Thus, alkalinity is only lost via the bleed stream, in Bio-FGD system, it requires a low input of lime or limestone.

In brief, apart from their importance in sulfur cycle, DSRs together with sulfur oxidizers can be successfully exploited in the sustainable clean-up of industrial waste streams.

Objectives

Hydrogen sulfide produced by sulfate reduction causes corrosion (Eq1) (Mattorano and Merinar, 1999).

$$Fe + 2H^{+} \rightarrow Fe^{2+} + H \qquad \text{(Eq 1)}$$

DSRs influence the equilibrium of this reaction, a process of microbially-induced corrosion. Hydrogen sulfide produced by sulfate reduction was also found to have direct and reversible toxicity effects on the physiology of DSRs (Reis et al., 1992). Knowing how to avoid hydrogen sulfide formation is highly important in biotechnological applications involving DSRs. In theory, the hydrogen sulfide produced by DSRs can react with iron on olivine surfaces, corrode the olivine and produce iron sulfides. It is unclear if microorganisms participated directly to this reaction, and whether this reaction will influence the growth of DSRs. The following hypotheses are proposed for this work:

1. The chemical reaction between the H_2S, produced by DSRs, and olivine is abiotic and it is not catalyzed.
2. The growth of DSRs will be positively influenced by the presence of olivine.

The mechanisms proposed to be involved in this process are summarized below:

Step 1 (Catalyzed by DSRs)

$4H_2 + SO_4^{2-} + 2H^+ \rightarrow H_2S + 4H_2O$ $\Delta G^{o'} = -152kJ/mol$

$R\text{-}COO^- + SO_4^{2-} + 3H^+ \rightarrow 2CO_2 + H_2S + 2H_2O$ $\Delta G^{o'} = -57.5kJ/mol$

where: $R = (CH_4)_X$

Step 2 (Abiotic process)

$Fe^{2+/3+} + H_2S \rightarrow FeS$

$Fe^{2+} + S^o + H_2S \rightarrow FeS_2$ (pyrite) $+ 2H^+$

Based on these objectives my work was divided in two parts:

1. Determine the equilibrium and rate of the chemical reaction between H_2S and olivine. Analyze the consumption of H_2S in the presence of olivine under various initial concentrations of H_2S. Investigate interferences produced by HCO_3^-, PO_4^{3-} and pH, which are some of the most common and wide ranging variables in sediments and culture media.
2. Verify the effect of olivine changes in cell density in DSR communities and identify species from the DSR communities.

Materials and methods

Olivine treatment

Table 3.1. gives size ranges and surface areas for olivine sands with two levels of granulation.

Table 3.1 Olivine particle sizes and BET surface areas.

Sieve size (um)	BET (cm^2 g^{-1})
250<d<420	307.0
149<d<250	598.0

Surface areas for Fo_{91} were measured by multi-point BET (Brunauer et al., 1938) using a krypton gas adsorption technique (Wogelius and Walther, 1992). Ground olivine with 0.4 mm particles diameter has a calculated surface area of about 7,000 mm^2/g. Because sands with smaller size olivine particles have larger surface area, it is expected that more finely ground olivine is better for studying the reaction between sulfide and olivine-iron. In our experiments, Fo_{90} olivine was crushed using a ceramic mortar and pestle and then size-fractioned using stainless steel sieves to minimize metallic iron contamination. The sand samples were sieved in the 150um-250um grain size range, washed with dH_2O and dried overnight in a 60^oC oven. In cultures, olivine was autoclaved in the growth medium. For chemical reactions non-sterilized olivine was used.

DSRs samples collection

Sediment samples were collected from the Willamette River (Portland, OR). This location is part of the Columbia River Basalt system. The samples were stored in the -40^{o}C refrigerator. A basalt slurry was transferred in a 2 mL microcentrifuge tube, and 100 uL of this slurry was used to inoculate olivine-containing culture media.

The Columbia River basalt (CRB) is a large igneous province that lies across parts of the Western United States, including Washington, Oregon, Idaho, Nevada, and California. Columbia River flood basalts are a series of ~300 stacked basalt flows that erupted between 6–17 million years ago (Alt and Hyndman, 1995). McKinley and Stevens (2000) analyzed microfossils from CRB and proposed that indigenous subsurface CRB microbial ecosystems persisted for millions of years. In 1995 and 1997 they have also reported that in the CRB area, paelosols contain methanogens, homoacetogens and DSRs and that along with sulfate and iron (III) reducers, H_2 is generated due to interaction between water and ferromagnesian silicates from basalt.

The chemical reaction experiment

We have prepared serial dilutions of H_2S (0.156mM, 0.313mM, 0.625mM, 1.25mM, 2.5mM from 50mM) from a 50 mM Na_2S solution adjusted to pH=7 and stored at -80^{o}C. The frozen Na2S bottles were melted in ice-water mixtures (0^{o}C) when needed. The serial dilutions were prepared in a oxygen-free glove box to avoid oxidation of the sulfide. The dH_2O used for this dilution was boiled and then purged with helium gas (He) for at least 24 hours. For each different concentration of H_2S, we have prepared six 2mL

centrifuge tubes, added 0.25g ground olivine to each tube, and 1mL from the serial dilution solution. The tubes were incubated at 37°C. Each sample also had a control which only contained 1mL of H_2S solution but without olivine.

We measured H_2S concentrations at the initial time, and then every 1.5h or 3h after incubation. For each measurement, we randomly took out one tube from each [H_2S] sample to measure changes in [H_2S]. During each sampling we have tested 10 different sample tubes and used six replicates for each measurement.

We have also prepared standard H_2S solution during each measurement to produce a standard line. The standard H_2S solutions contained 0mM, 0.156mM, 0.313mM, 0.625mM, 1.25mM, 2.5mM and 5mM H_2S.

Hydrogen sulfide is slightly soluble in water and as a weak acid, it can be ionized to produce bisulfide (HS^-) (pK_a = 6.9 in 0.01-0.1 mol/L solutions at 18 °C) and sulfide (S^2) (pK_a = 11.96). However, sulfides are not detected far from their source areas, or long after collection, due to their high reactivity with O_2. Therefore, rapid measurement of H_2S is desirable immediately after sampling. A number of techniques have been developed to measure total sulfide species (H_2S, HS^-, S^{2-} and polysulfides). These include colorimetric methods with methylene blue, nitroprusside and nitrilotriacetic acid and iron (Guenther, 2001). In this study we have used the diamino methylene blue method, which needed DPD reagent and 30mM $FeCl_3$ acid solution. The DPD reagent was prepared by mixing 119mL concentrated HCl (12.1M HCl), 81mL dH_2O and 0.938g of N,N-dimethyl-p-phenylene-diamine sulfate. Acid solution of 30mM $FeCl_3$ was prepared by mixing 20mL concentrated HCl, with 180 mL dH_2O and 1.62g $FeCl_3.6H_2O$.

For each measurement, we took samples very fast by avoiding air as much as possible, because sulfides would react with oxygen in a couple of seconds. All reactions have occurred in the glove box in the absence of air. In centrifuge tubes we have mixed 10uL DPD reagent (20mM Diamino dissolved in 7.2N HCl), 100uL sample containing sulfides, mixed gently, rapidly added 10uL of the 30mM $FeCl_3$ solution, vortexed again and incubated in the dark for 20min. The samples were distributed in six replicates in 96-well plates, and absorption at 650nm was measured using a microplate spectrophotometer (8452A; Hewlett Packard). Using the H_2S standards, we have produced equations representing the relationship between the concentration of H_2S concentration and absorbance at 650nm in each sample

The effect of [HCO_3^-] on the reaction

We have prepared different concentrations of HCO_3^- (0mM, 10mM, 20mM and 50mM) by diluting from a 1M Na_2CO_3 solution. Each [HCO_3^-] sample had a control which contained 1mL 2.5mM H_2S and different [HCO_3^-]. Some sample tubes also contained 0.25g of ground olivine, as needed. We have used five centrifuge tubes for each sample and for each control, so the total number of centrifuge tubes for testing in each experimental series was 40.

After adding 1mL of different HCO_3^- solutions (pH=7) to each tube, plus 0.25g ground olivine, we left these tubes in the glove box for 24h to let the olivine react with the solution completely. Next day, we have injected 40uL 50mM H_2S in each tube (still in the glove box) and measured the [H_2S] as shown above at initial time and then every

1.5h until 6 hours of incubation. For each time measurement series, we randomly took out one tube representing a different [HCO_3^-] sample and measured the results. Thus, every time we made a series of measurements we have verified 8 different tubes representing various times of incubation (0h, 1.5h, 3h, 4.5h and 6h).

The effect of pH on the reaction

With regard to pH effects two experiments have been performed:

a. We have prepared three different pH solutions with (pH = 5, 7 and 9) using a Thermo Orion pH meter model 410, and adjusted the solutions' pH with HCl or NaOH solutions. Each pH sample had a control containing 1mL of 2.5mM H_2S. In the sample tubes we have also added 0.25g of ground olivine. We prepared five 2mL centrifuge tubes for each sample and for each control, to a total of 30 centrifuge tubes in each series. After adding 1mL different pH solution to each tube and the 0.25g ground olivine in the sample tubes, we incubated these tubes in the glove box for 24h to let the olivine react with solution completely. We have injected 40uL of 50mM H_2S in each tube (still in the glove box), measured [H_2S] as shown above at the initial time and then after 2, 4 and 6 hours of incubation. For each time interval, we randomly took out one tube from each different sample and made H2S measurements. Each sample was tested in six replicates.

b. We have prepared three different pH solution (pH = 5, 7 and 9) as shown above. For this experiment we have used 140 ml serum bottles. Each pH sample had a control containing 50mL of 2.5mM H_2S and 12g ground olivine. In total six 140 mL bottles were used in each series of measurements. Each sample bottle contained 12g ground olivine.

All bottles were incubated for 24h in the glove box prior to adding the H_2S. We injected 2.5mL 50mM H_2S per bottle in glove box, measured pH with a pH meter at the initial time, and then after 1.5h, 3h, 4h and 6h of incubation. All preparations and measurements were made in an O_2-free glove box.

The effect of [PO_4^{3-}] and [NH_4^+] on the reaction

We prepared different concentrations of PO_4^{3-} samples (0mM, 5mM and 10mM) by diluting from a 1M Na_2HPO_4 solution, then mixed with one of two concentrations of NH_4^+ (0mM and 10mM) by dilution from a 1M NH_4Cl solution. Each sample had a control with 1mL of 2.5mM H_2S and various [PO_4^{3-}] and [NH_4^+]. The samples also contained 0.25g ground olivine. We have prepared four centrifuge tubes for each sample and control, to a total of 40 centrifuge tubes per series. After adding 1mL mixed solution of PO_4^{3-} and NH_4^+ (pH=7) to each tube, 0.25g ground olivine was added as needed, and the tubes were incubated in the glove box for 24h to allow the olivine to react with the solution to completion. Then we injected 40uL of 50mM H_2S in each tube (still working in the glove box), measured [H_2S] at the initial time and after, 2h, 4h and 6h of incubation. For each time interval we randomly took one tube and used it for measurements.

The effect of [PO_4^{3-}] on the reaction

We have prepared different concentrations of PO_4^{3-} samples (0mM, 5mM, 25mM, 50mM and 100mM) by diluting from a 1M Na_2HPO_4 solution. Each [PO_4^{3-}] sample had a control containing 1mL of 2.5mM H_2S and different [PO_4^{3-}]. Sample tubes also

contained 0.25g ground olivine. We have prepared four centrifuge tubes for each sample and for each control to a total of 40 centrifuge tubes for each test series.

After adding 1mL of different PO_4^{3-} concentration solutions (pH=7) to each tube and 0.25g ground olivine to all sample tubes, the tubes were incubated in the glove box for 24h to allow olivine to react with solution completely. Next day, we have injected 40uL of 50mM H_2S per tube (still in the glove box) and measured the [H_2S] at the initial time and then after 2h, 4h and 6h of incubation. For every time measurement, we randomly took out one tube of each [PO_4^{3-}] and measured [H_2S]. For each time interval we have tested ten different tubes.

Isolate DSRs capable of oxidizing LASP from olivine-containing enrichments

The mineral medium used for culturing isolation contained (per liter) 1mL trace mineral solution, 1mL vitamin mix, 30 mmol phosphate buffer (pH 7), 20 mmol bicarbonate, 30 mmol nitrate, and 100 g ground olivine. The trace mineral solution contained 5.6mM H_3BO_3, 1mM NaCl, 0.54mM $FeSO_4$, 0.5mM $CoCl_2$, 0.5mM $NiSO_4$, 0.39mMNa2MoO_4, 0.15mM $NaSeO_4$, 0.13mM $MnCl_2$, 0.13mM $ZnCl_2$ and 0.02mM $CuCl_2$. The vitamin mix solution contained (per milliliter) 5 ug p-aminobenzoic acid, 5 ug biotin, 5 ug cyanocobalamin, 5ug folic acid, 100 ug i-inositol, 100 ug nicotinic acid, 100 ug pyridoxine, 100 ug panthotenic acid, 100 ug riboflavin, and 1 ug thiamine. The vitamin mix was added filter-sterilized after autoclavation. All chemicals were reagent grade. The mineral medium solution contained 10 mMNa_3PO_4, 1 mM $NaHCO_3$, 0.05 mM $MgCl_2$, 0.05 mM $CaCl_2$, 0.05m MKCl and was adjusted to pH 7.0.

We have inoculated roll tubes with a serial diluted sample originating from Willamette river sediments. In each Hungate tube we have added 5mL of organic mixture medium (10mM Pyruvate, 20mM Succinate, 20mM Lactate, 50mM Acetate, 10 mL/L Wolfe vitamins, 4mM $(NH_4)_2SO_4$, 100uM $FeCl_3$, 2% agar). All tubes were sealed with a butyl rubber stopper and crimped. Then, we injected 100uL inoculum in the first tube and 100uL inoculums in the rest of tubes. We incubated the roll tubes horizontally, and verified the formation of black colonies at one week intervals. The LB plates used for DSRs isolation contained 32 g/L LB agar. Colonies picked up from the roll tube were streaked on the LB plates to determine whether any of the isolates were also heterotrophs. After 7days of incubation about, the colonies with dissimilar morphology were selected for DNA extraction and phylogenetic identification.

DNA-based sequencing

We have prepared bottles with 50mL liquid medium for sulfate reducers (10mM Pyruvate, 20mM Succinate, 20mM Lactate, 50mM Acetate, 0.5% L-cysteine, 5% yeast extract and 4mM $(NH_4)_2SO_4$). After autoclavation, we have injected each bottle with H_2 for 15minutes, 1mL/Lvitamin mix was added filter-sterilized and 200uL inoculums was added from LB medium isolates. For inoculation from colonies we have used sterilized toothpicks and selected colonies with dissimilar morphologies from the LB plates. A total of eight colonies were selected. We have incubated the culture tubes at 30^{o}C in the glove box for 7days. Cells were separated by centrifugation (7,500g, 10 min at 20^{o}C) and the cell pellets were used for DNA extraction.

To extract genomic DNA we have used a direct hot TE extraction method directly from cell pellets (modified after de Bruijn, 1992; cited in Siering and Ghiorse, 1996; Emerson and Moyer, 1997; Mazza et al., 2003). Then we have added 1 mLof 1X TE buffer (pH 8; 10 mM Tris/HCl; 1 mM EDTA). After vortexing, we transferred the suspension in two 1.5 mL polypropylene centrifuge tubes and centrifuged for 2 min at 7,500g. The cell pellets were washed once with 500 uL of 1X TE buffer and vortexed well. After resuspending the cells in 500 uL of TE buffer, we placed the tubes over boiling water for 10 min. The tubes were then cooled for 5 min and centrifuged for 3 min at 7,500 g to eliminate cellular debris and mineral particles. We transferred, with a pipette, 420 uL of the supernatant to a clean tube and stored it at 4^{o}C. Next step was DNA cleaning and the elimination of eliminating inhibitors. To achieve this we have added 980 ul isopropanol to each tube (to a final concentration of 70% isopropanol), and flipped the tubes gently 30-40 times to precipitate the genomic DNA. The tubes were then centrifuged (20 min, 14,000 g, 1.5^{o}C) and the pellet was washed twice with cold (-40^{o}C) 70% EtOH. The concentration of gDNA was quantified with a NanoDrop 1000 spectrophotometer.

16S rDNA amplification by PCR was prepared as follows. The concentration of all samples was adjusted to 50ng/ul, then PCR reactions were prepared in 20ul final volumes (10ul of 2X PCR mix (Fermentas); 0.8ul of 10 uM 8F forward primer (5'AGAGTTTGATCCTGGCTCAG); 0.8ul of 10 uM 1492R reverse primer (5'GGTTACCTTGTTACGACTT) (Baker et al., 2003); 1uL of 0.5ug/uL bovine serum albumin (BSA) and 7.4uL of 50 ng/uL gDNA template). In the control tube we have

replaced the gDNA template with 7.4uL nuclease free H_2O (Fermentas). For all PCR amplifications we have used a PCR kit (Fermentas) and a GeneAmp 2400 thermocycler (Perkin Elmer). The PCR conditions were: denaturing 95^{o}C for 15 min; 45 cycles of 95^{o}C for 30sec, 52^{o}C for 1min. and 72^{o}C for 2min; and final extension 72^{o}C for 5min. The size of the PCR products was verified by 0.7 % agarose electrophoresis at 120V for 30min. 10µL of PCR products were cleaned with an UltraClean PCR DNA purification kit (MoBio, G-3148-250). After purification, we have quantified the PCR products using a Nanodrop. The DNA concentration was brought to a concentration of about 17.4 ng/ul. Amplicons were sequenced at the DNA Sequencing Core facility of Oregon Health and Sciences University using three primers: 8F, 515F (5'-GTGCCAGCMGCCGCGGTAA) and 1492R (Baker et al. 2003) by capillary electrophoresis on an ABI 3130xl instrument. Duplicate sequences were manually aligned, and when differences between duplicates were found we repeated the PCR and sequencing to compare triplicates for each sequence. The sequence of each isolate were assembled into contiguous DNA fragments and blasted in the Ribosomal Database for phylogenetic identification.

The effect of olivine on the growth of DSRs

We have prepared six 140mL bottles with 50mL solution, using triplicate for each sample and control. The sample bottles contained 50mL solution made from mineral medium (pH=7), 10g ground olivine, 10mMNaH_2PO_4, 4mM$(NH_4)_2SO_4$, LASP(10mM Pyruvate, 20mM Succinate,20mM Lactate, 10mM Acetate), 2.5g/L yeast extract, 0.1g/L L-Cysteine (used as an antioxidant). We adjusted the pH to 7 using a pH meter, sealed

with a rubber stopper and crimped with an aluminum seal. The bottles were filled with N_2 (containing 1.6% O_2), autoclaved and cooled off. The vitamin mix was added filter-sterilized at a final proportion of 1mL/L. The preparation for control bottles was similar, except that olivine was not added. We injected 200uL of isolated DSRs inocula to each bottle in the glove box, and incubated all samples and controls with stirring (150 rpm) at room temperature.

We did cell counting every day by using live/dead cell stain (Baclight bacterial viability kit, Invitrogen) and acridine orange stain. For these observations we have extracted and vortexed 400uL of from each culture the bottles a different time intervals. We have added 900uL of PBS buffer in 3 microcentrifuge tubes and labeled them 10^{-1} to 10^{-3}. We added 100uLof culture to the 10^{-1} tube, vortexed very well for ~10seconds and continued with the serial dilution down to 10^{-3}. Using forceps, we placed polycarbonate 0.2 um filters (Poretics) on a vacuum funnel and filtered 1mL of the 10^{-3} dilution on each filter. For staining with acridine orange we have added 100ul 1X acridine orange solution in PBS buffer. The filter tower was covered with aluminum foil to avoid exposure to light and incubated in the dark for 5 minute. The cells were washed with PBS and the filters were observed by epifluorescent microscopy at 1000X magnification. We have counted the cells from five microscope fields and calculated averages. Using the formula below we calculated the density of cells per mL:

Number of cells/mL= (Average cell count * X *11053)/Y

X=1mL (the volume of cell suspension filtered)

11053= the approximate number of fields on the filter when the 1000X magnification is used.

Y= the dilution factor (10^{-3}, etc)

Results

H_2S/olivine chemical reaction

Fig 3.3 illustrates the relationship between the concentration of H_2S ([H_2S]) and 650nm absorbance in the methylene blue method. These standard solutions we have used were based on seven data points (0mM, 0,156mM, 0.313mM, 0.625mM, 1.25mM, 2.5mM, 5mM H_2S). For this application, we have used an order 2 polynomial fit. In order to obtain the large R-squared value shown in Fig. 2.2 six replicates had to be used for each measurement and [H_2S]. Because H_2S is highly sensitive to oxidation and the methylene blue reactions gives different curves in different days we have created new standards for each series of measurements.

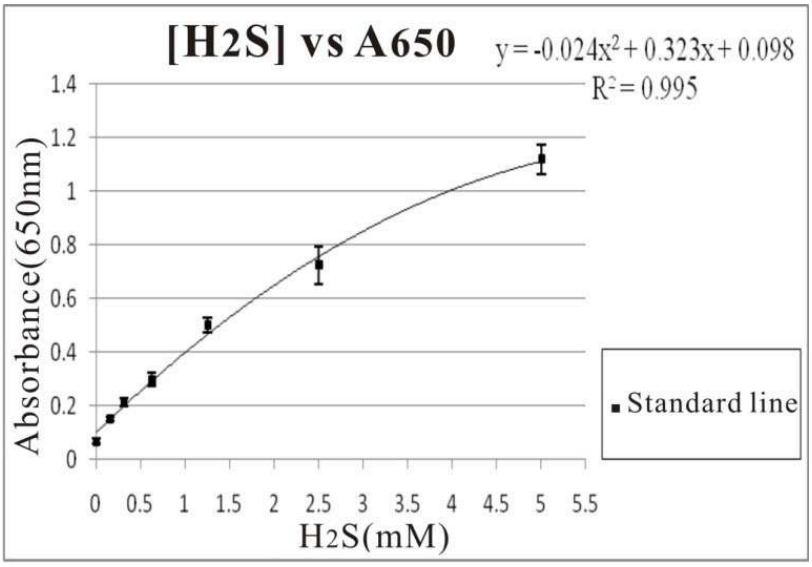

Fig 3.3. Example of standard curve used to determine the concentration of H_2S with the methylene blue method.

To obtain the results for the H_2S/olivine chemical reaction (such as the example from Fig 3.4), we prepared triplicate of controls and samples in centrifuge tubes with 4mM H_2S and measured the [H_2S] concentration after 0h, 2h, 4h, and 24h of incubation. The [H_2S] dropped in time in controls as well. After 24h the final [H_2S] in controls was about 2mM. This was attributed to slow oxidation of H_2S with traces of O_2 from the gas phase and to loss of H_2S from the liquid phase by evaporation. The [H_2S] in the sample tubes dropped fast in the first 4 hours from 4mM to about 1.5mM, then this rate slowed down for the remaining 20 hours until the [H_2S] reached zero with regard to the methylene blue method.

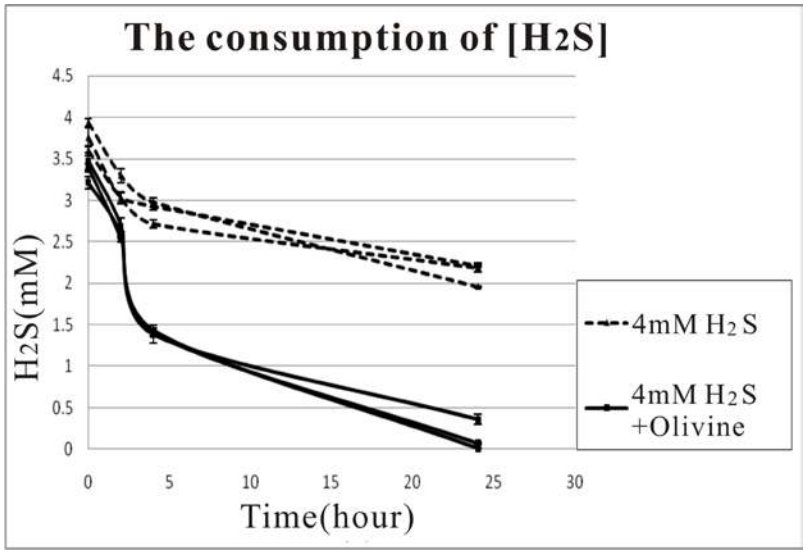

Fig 3.4. The consumption of H_2S in the liquid phase during 24h of incubation with and without olivine. The error bars are standard deviations based on six replicate measurements of each sample and control.

The reaction between H_2S and olivine iron produces a black precipitate rich dominated by amorphous FeS and causes the consumption of H_2S. During incubation, a black precipitates can be observed on olivine surfaces. Based on results such as those from Fig. 3.4 we have seen that the fastest and most important part of the reaction between H_2S and olivine iron occurred in the first 4 hours. Thus, for the next step we have shortened the incubation time to 8.5 hours, and measured the H_2S concentration at 1.5 hour intervals. One example of such results is shown in Fig 3.5.

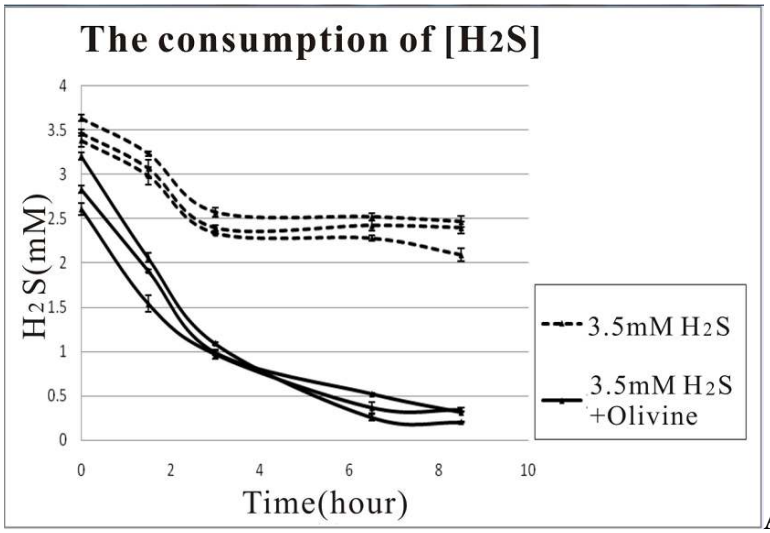

A

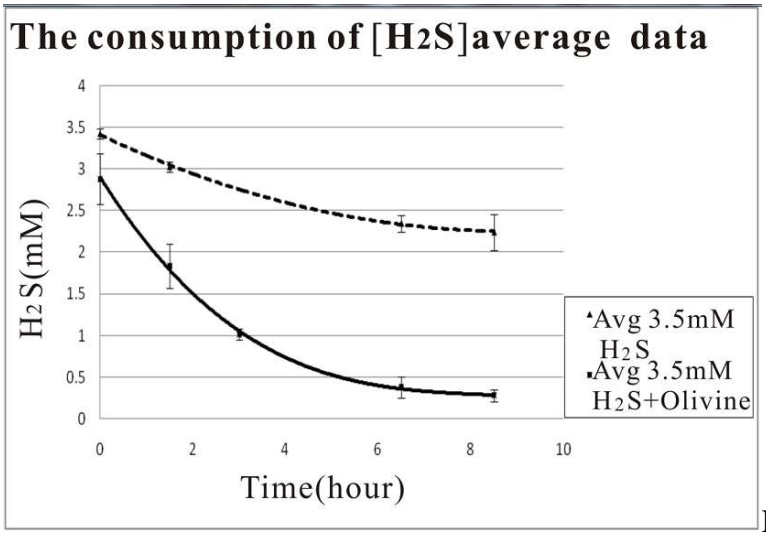

B

Fig 3.5. The consumption of H_2S concentration in liquid phase during 8.5 hours of incubation w/wt olivine present. Graph A. Six separate readings comparing the consumption of H_2S with and without olivine present. Graph B. Plots comparing the consumption of H_2S with and without olivine based on averages from Graph A ploted by usign polynomial equations. The error bars from Graph A are standard deviations based on six replicate measurements of each sample and control. The error bars on B are standard deviations based on the triplicate readings from Graph A.

We have prepared tripliate control and sample tubes with an initial H_2S concentration of about 3.5mM. Each sample tube contained 0.25g gound olivine while the control tube contains no olivine. We measured the [H_2S] after 0h, 1.5h, 3h, 6.5h and 8.5h of incubation. Results have shown that the [H_2S] in control tubes has dropped smoothly to about 2mM after 8 hours of incubation (Fig. 3.5). The [H_2S] in the sample tubes dropped fast to 1.0 mM in the first 3 hours. Then, this consumption rate decreased until most H_2S from the liquid phase has been consumed. The reaction between H_2S and olivine iron was considered to be primarily responsible for the consumption of H_2S, and the rate of this reaction was faster in the first 4hours.

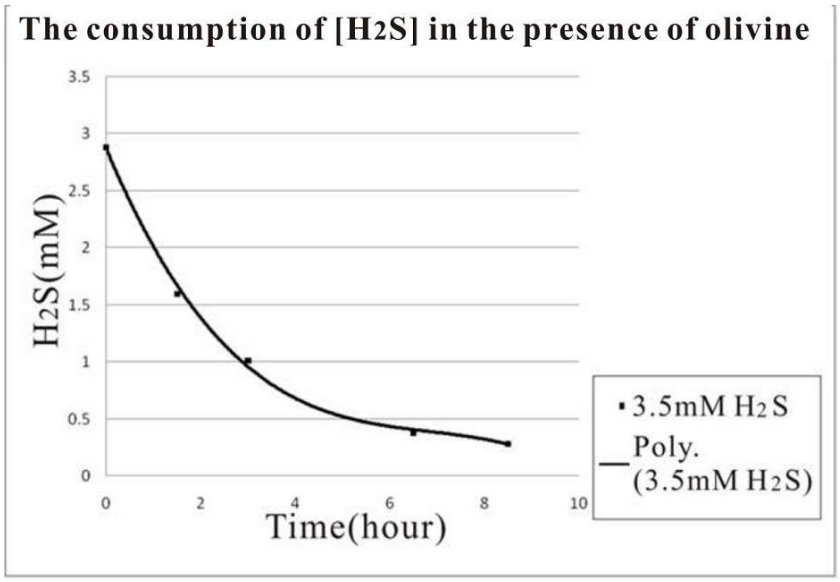

Fig 3.6. The evolution of net consumption of H_2S from the liquid phase due to reaction with olivine iron. The plot shown in this figure was obtained by subtracting results of incubating H_2S without olivine from results of incubating H_2S with olivine. Each initial measurement used to obtain results was based on six replicates (similar to Fig. 3.5).

Using results such as those from Fig 3.5, we have corrected the H_2S concentraion data in the sample tubes. This subtraction eliminated the oxidation of H_2S with O_2 traces from the gas phase or to H_2S evaporation (Fig. 3.6). Based on this corrected curve, the bulk of the reaction between H_2S and olivine iron happened in the first 3 hours of incubation. After about 8 hours, this reaction reached near full completion with regard to the sensitivity of the methylene blue method.

For the next series of experiments we have prepared serial dilutions of H_2S, incubated in centrifuge tubes and compared the H_2S consumption rate starting from various initial [H_2S] (Fig 3.7).

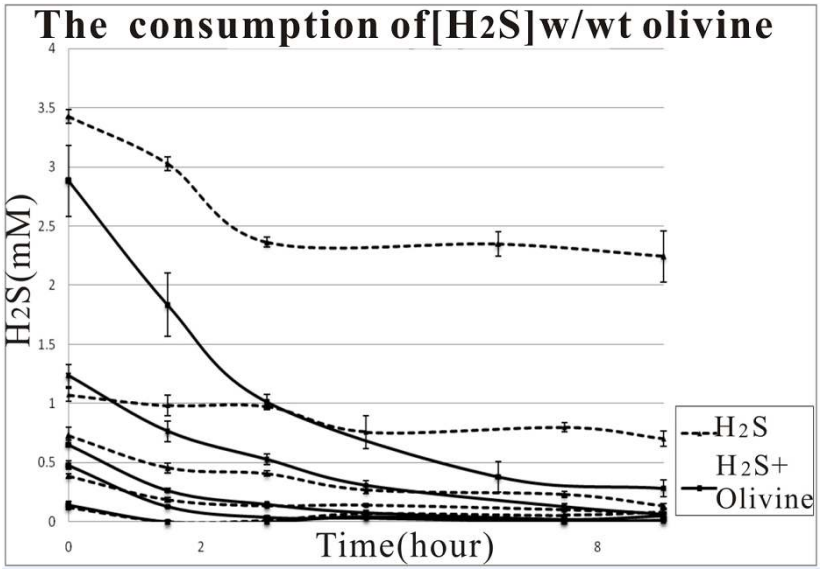

Fig 3.7. The evolution of the consumption of H_2S w/wt olivine starting from various [H_2S]. The error bars are standard deviations based on six replicate measurements of each sample and control.

For better understanding of the relationship between the H_2S consumption rate and the initial H_2S concentration, we have prepared serial dilutions containing

0.156mM,0.313mM, 0.625mM, 1.25mM and 2.5mM H_2S. We have measured H_2S concentrations after 0h, 1.5h, 3h and 9h of incubation when the [H_2S] reached about 0mM. To analyze the effect of the initial [H_2S] on the H_2S consumption rate, we have corrected the changes as shown in Fig. 3.6. An example of such corrected data is shown in Fig 3.8.

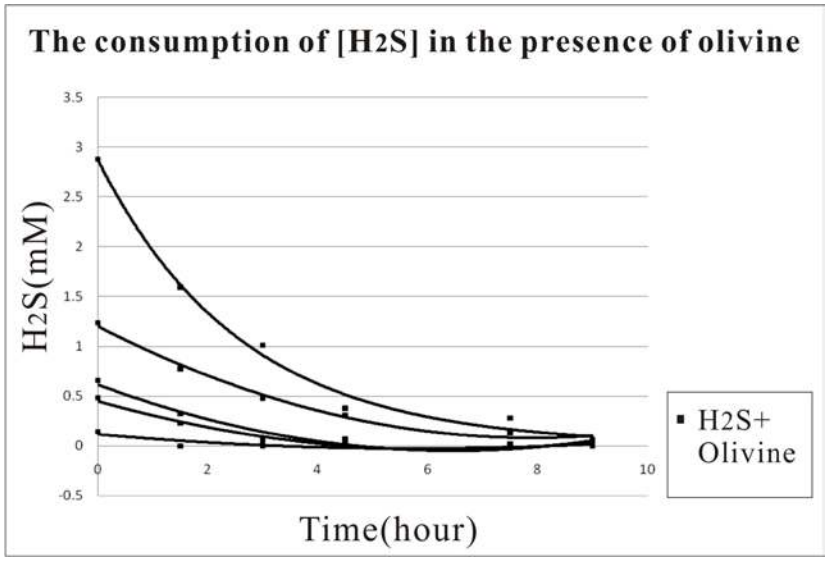

Fig 3.8. The effect of the initial [H_2S] on the evolution of [H_2S] during reaction with olivine. The data shown in this graph are based on differenes between samples and controls (Fig. 3.7), similar to the analysis from Fig. 3.6.

Fig 3.8 was corrected based on data from Fig 3.7. Results indicate that the reaction rate was faster, and most of the reaction occurd in the first 3 hours of incubation. As expected, the initial rate was faster when the [H_2S] was larger. Eventualy, after 9 hours, the [H_2S] was similar amog all samples. In order to determine the relationship

between H_2S consumption and the initial $[H_2S]$, we have calculated the initial rates of H_2S consumption, and plotted them as shown in Fig 3.9.

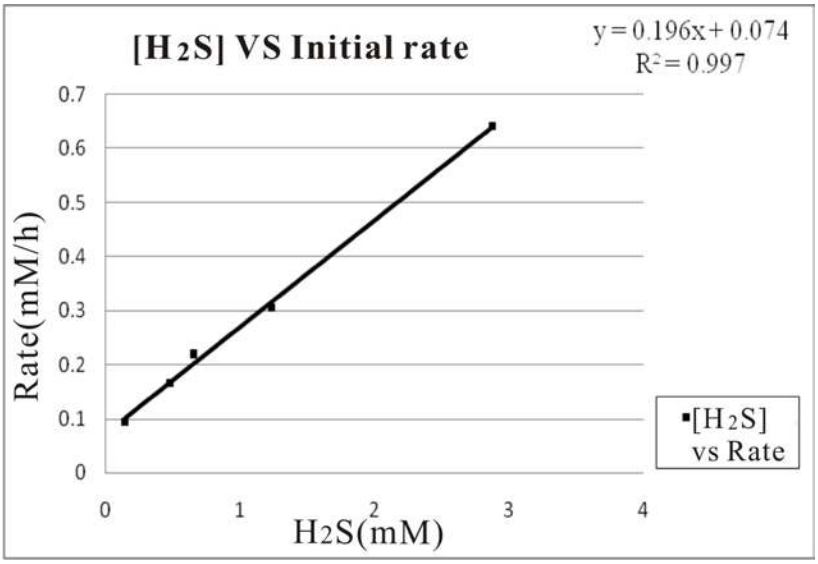

Fig 3.9. The relationship between the initial $[H_2S]$ and the initial H_2S consumption rate. This plot is based on results from Fig. 3.8.

Fig 3.9, calculated based on data from Fig 3.8, showed the relationship between the initial $[H_2S]$ concentration and the initial consumption rate of H_2S. These readings were based on five initial $[H_2S]$ values: 0.14mM, 0,48mM, 0.65mM, 1.2mM and 2.8mM H_2S. The initial consumption rate calculated from:

$V = ([H_2S]^0 - [H_2S]')/t.$

$[H_2S]^0$ is Initial H_2S concentration

$[H_2S]'$ is H_2S concentration after 2 hours

t is time (2hours)

Using the results from Fig. 3.9 we have produced a linear equation explaining the effect of [H_2S] on the reaction rate between H_2S and olivine iron.

$Y=0.196X+0.074$ ($R^2 = 0.997$).

where: Y is initial rate and X = [H_2S]

Based on results such as those from Fig 3.9, we have determined the relationship between the initial reaction rate and [H_2S]. This can be used to analyze the order of the reaction. The order of a reaction tells us about the functional relationship between concentration and rate and determines how the amount of a compound speeds up or retards a chemical reaction. The order of a reaction is simply the sum of the exponents of the concentration of reagents:

Rate = $k[A]^x[B]^y$ reaction order = x + y

Based on the different sum of exponents, the reaction can be zero order, first order, seconder order, mixed order, or negative order. In our experiment, the rate was linearly correlated with the [H_2S] when olivine was not limiting. Based on these we propose that this is an abiotic first order reaction. Based on these results we find no reason to suspect that this reaction has to be catalyzed by bacteria and in incubations of DSRs with olivine the formation of iron sulfide precipitates is most probably an example of passive (or induced) biomineralization.

Although the chemical reaction between H_2S and olivine is a first-order reaction, and the rate is primarily influenced by the [H_2S], some other factors from nature of

culture media may still influence this reaction. We have analyzed the effect of three such factors: pH, bicarbonate and phosphate.

The effect of [HCO_3^-], [PO_4^{3-}] and pH on the reaction

Fig 3.10 shows the effect of bicarbonate concentration [HCO_3^-] on the chemical reaction between H_2S and olivine. Bicarbonate is the result of deprotonating carbonic acid or a conjugate acid derived from CO_3^{2-}.

$$H_2CO_3 + 2H_2O \rightleftharpoons HCO_3^- + H_3O^+ + H_2O \rightleftharpoons CO_3^{2-} + 2H_3O^+$$

$$CO_3^{2-} + 2H_2O \rightleftharpoons HCO_3^- + H_2O + OH^- \rightleftharpoons H_2CO_3 + 2OH^-$$

Bicarbonate is used to produce pH buffers, in conjunction with water, hydrogen ions and carbon dioxide. Bicarbonate is also commonly used in culture media for DSRs. In the DSR growth experiments used in this study we have used about 1 mM HCO_3^-.

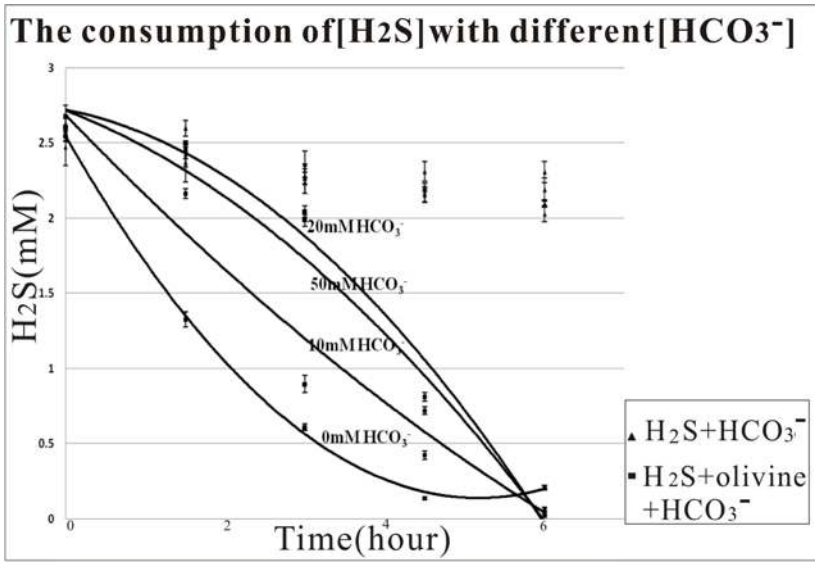

Fig 3.10. The consumption of H_2S in the prescene of varius [HCO_3^-]. These chemcial reactions have occurred after bicarbonate was initially incubated with olivine for 24 hours (see: Materials and methods). The error bars are standard deviations based on six replicate measurements of each sample and control.

For these experiments we have used serial dilutions of HCO_3^- (0mM, 10mM, 20mM and 50mM). Before making H_2S/olivine reaction experiments 0.25 g of olivine has been incubated in anaerobic conditions with 1 ml of media containing bicarbonate at pH 7.0 for 24 hours. After 24 hours of incubation, we have injected 40ul of 50mM H_2S in each tube (inside the glove box) and measured the [H_2S] at time zero and at 1.5 h intervals.

When the initial [HCO_3^-] was 0mM, the sharpest drop in [H_2S] has occurred in the first 3 hours of incubation. In the first three hours the H_2S consumption rate was negatively correlated with the [HCO_3^-] in the range 0mM to 20Mm. The trend line of

H_2S change was yet similar between 20mM HCO_3^- and 50mM HCO_3^-. After 6 hours of incubation, the [H_2S] dropped to near 0mM in all samples irrespective of the [HCO_3^-].

Based on these results, our working hypothesis is that "Bicarbonate inhibits the reaction between H_2S and olivine, but does not change the final equilibrium". The negative correlation between bicarbonate concentration and H_2S consumption during the first three hours is attributed to HCO_3^- reacting first with olivine iron, producing amorphous iron carbonates or siderite on olivine surfaces, thus temporarily blocking the reaction between H_2S and iron. The predicted chemical reaction is shown below:

1. During early reaction during the incubation of olivine with bicarbonate in the oxygen-free glove box for 24hours.

   $2HCO_3^- + Fe\ (II) \Rightarrow Fe\ (HCO_3)_2 \Leftrightarrow Fe^{2+} + 2HCO_3^-$

2. The equilibrium shown below indicates the relationship among solutes (ferrous bicarbonate) and aquifer minerals (siderite) in this system. Siderite (ferrous carbonate) is often associated with calcite, especially in sedimentary rocks, and may be a likely solid phase in carbonate-rich rocks when the environment is relatively reducing. These conditions should be relatively common in ground-water aquifers (Hem, 1960).

   $Fe^{2+} + HCO_3^- \Leftrightarrow FeCO_3$ (siderite) $+ H^+$

   The equilibrium constant for this reaction, calculated based on free-energy results, is 0.46 (Latimer 1952).

3. We assume that siderite has covered the olivine surfaces, blocking the reaction between H_2S and iron. But this unstable mineral (i.e. siderite) can react with dissolved H_2S in aqueous solution producing amorphous iron sulfide. This causes consumption of hydrogen sulfide.

$FeCO_3 + H_2S \Rightarrow FeS + H_2CO_3$ (amorphous FeS)

The next logical step was to analyze the H_2S consumption rate during reaction with olivine when bicarbonate was also present.

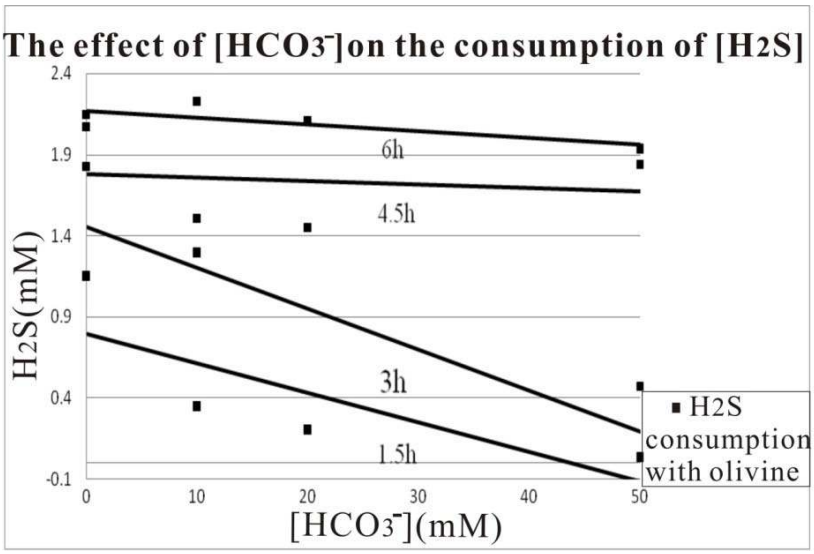

Fig 3.11. Example of results showning the evolution of H_2S during reaction with olivine in the presence of various bicarbonate concentrations.

In order to produce the results shown in Fig 3.11, we have subtracted the H_2S consumed in the control experiments. Results showed that when the concentration of bicarbonate was larger the reaction of H_2S with olivine was stronger. With increased

incubation time, the H_2S concentrations became positively correlated with the bicarbonate concentration, most likely due to the reaction between siderite and H_2S. Large amounts of siderite produced led to more H_2S to be consumed after 3hour incubation, until all the H_2S dissolved in the solution has been consumed. These results were confirmed in repeat experiments.

For the next series of experiments we have focused on the influence of pH on the reaction between H_2S and olivine. Fig 3.12 shows the H_2S consumption after 0h, 2h, 4h and 6h of incubation. Based on our initial results, changes in the reaction between H_2S and olivine were not significantly influenced by pH in the range pH 5 to pH 9. This wide pH range is beyond the expected variation of pH in our experiments and during DSR incubations. The [H_2S] has decreased in experiments with olivine as expected from earlier experiments (Fig. 3.12).

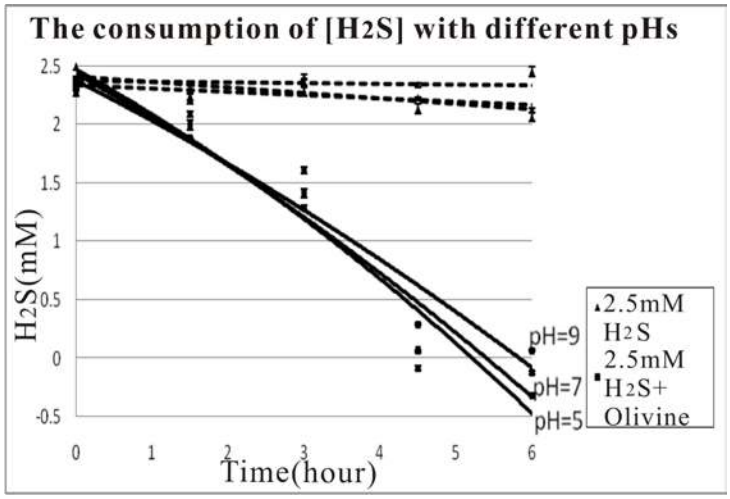

Fig 3.12. The consumption of H_2S at varius pHs with and without olivine.

Next we have studied changes in pH during the H_2S/olivine chemical reaction (Fig. 3.13). In this experiment, we have measured the pH with a pH meter after 0h, 1.5h. 3h, 4.5h and 6h of incubation. For each sample we have used controls with similarly treated composition and without olivine. These measurements were made in an oxygen-free glove box to avoid H_2S from being oxidized.

Based on the pH results we have calculated proton concentration in solution using:

$pH = -\log [H^+]$

$[H^+] = 10^{-pH}$

where: [H+] is the concentration of hydrogen ions in mol/L

Based on our results, the pH has changed little ($d[H^+] = \pm 0.1$mM) during the reaction between H_2S and olivine. Both Fig3.12 and Fig 3.13 indicate that the reaction between H_2S and olivine was not influenced by acidic or alkaline solutions, and that the pH was relatively stable during this reaction. Although the pH did not interfere in this reaction, to keep al experiments similar we used an initial pH of 7 in all experiments including DSR incubations. Reis (1992) has measured the effect of pH on the growth rate of sulfate reducing bacteria in the range pH 5.8 to 7.0 and found largest growth rate at pH 6.7 (Reis et al. 1992).

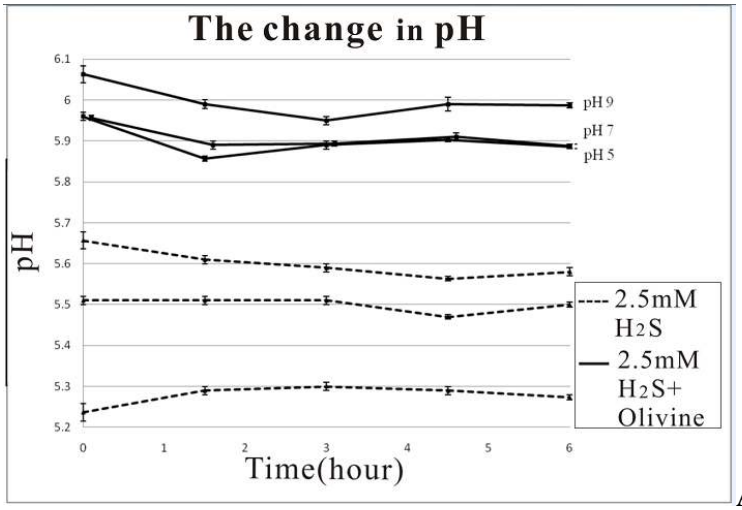

A

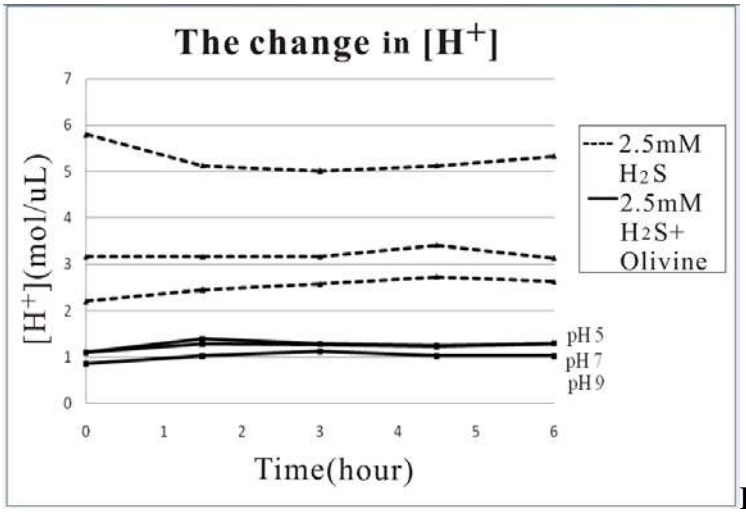

B

Fig 3.13. The changes in the pH and protons concentration during the incubation of H_2S solution with and without olivine. Graph A: the change of pH during the reaction. Graph B: the evolution of protons concentration, calculated from resutls shown in graph A.

For the next step we have analyzed the effect of PO_4^{3-} and NH_4^+ on the reaction between H_2S and olivine. Phosphate salts that are commonly used in pH buffer solutions. In my experiments, the concentraion of phosphate was 10 mM in the mineral medium used for cell growth. The ammonium ion is mildly acidic and is also present in DSRs

culture media. We have injected 4mM $(NH_4)_2SO_4$ in culture media so that the final concentration of ammonium was 8mM.

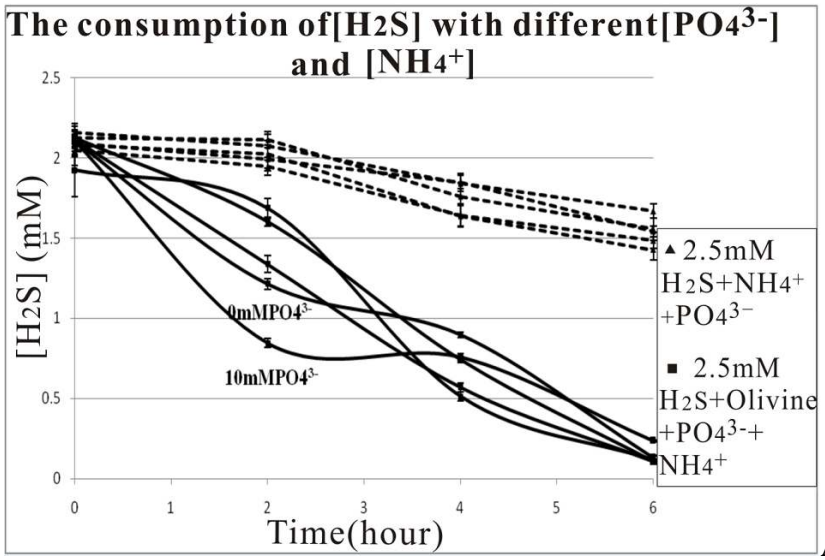

A

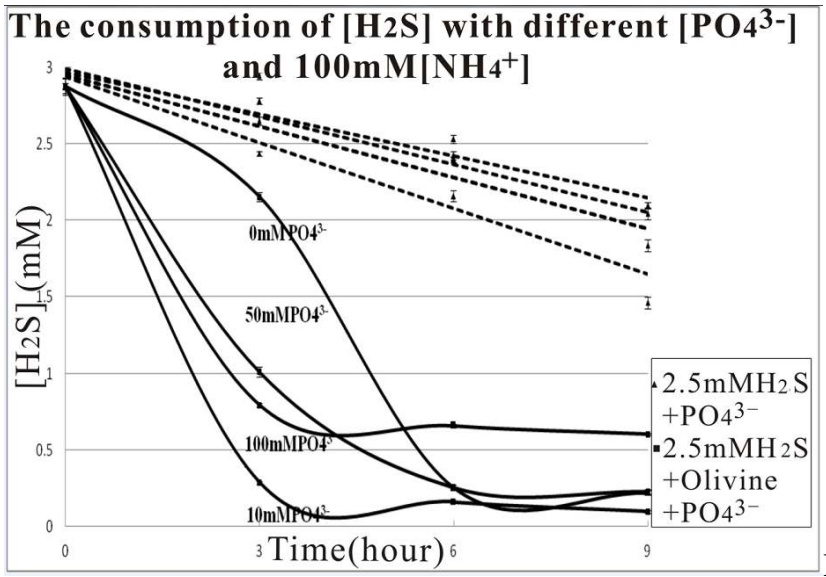

B

Fig 3.14. The evolution of H_2S in the presence of various PO_4^{3-} and NH_4^+ concentrations when olivine was present and absent. A: Evolution of H_2S in the presence of 100mM NH_4^+ and various concentrations of PO_4^{3-} (0mM, 10mM, 50mM and 100mM). B: Evolution of H_2S with two concentrations of PO_4^{3-} (0mM and 10mM) and to

concentrations of NH_4^+ (0mM and 10mM). The error bars are standard deviations based on six replicate measurements of each sample and control.

We expected to see that when PO_4^{3-} and NH_4^+ were present in the presence of olivine their reaction with Mg loosely bound on olivine surfaces and produce small amounts of struvite precipitate ($NH_4MgPO_4 \cdot 6H_2O$). Struvite is soluble in acid conditions but less soluble in neutral and alkaline conditions. We assumed that if struvite was formed, it should inhibit the reaction between H_2S and olivine.

From Fig. 3.14 it can be seen that the concentration of H_2S in controls, which contained various concentrations of phosphate and ammonium but no olivine, only decreased by 1mM. This decrease in H_2S concentration was attributed to chemical oxidation. In samples, which contained olivine as well, the fastest H_2S consumption in the first 3 hours occurred with 10mM PO_4^3 and 0m NH_4^+. On the contrary, the slowest H_2S consumption in the first 3 hours occurred with 100mM NH_4^+ and 0mM PO_4^{3-}. After 6 hous, the [H_2S] reached 0mM in all samples.

The results did not support the initial *struvite hypothesis* that both phosphate and ammonium have to be present to inhibit the reaction between H_2S and olivine. Based on Fig 3.14 , it can be deduced that PO_4^{3-} and NH_4^+ do not react with Mg from olivine surfaces to make measurable amounts of struvite. This is consistent with earlier reports that the formation of magnesium ammonium phosphate on olivine surfaces with phosphate and ammonium from solution requires acidification and high temperature conditions, 90~100^{0}C (MacIntire and Marshall, 1959)

Because the fastest consumption of H_2S in the first 3 hours happened in the presence of 10mM PO_4^{3-} without NH_4^+ present, the next step was to investigate the consumption of H_2S in the presence of olivine with various concentrations of phosphate. The solid lines from Fig 3.15 represent the evolution of [H_2S] in samples with various concentrations of phosphate and with olivine present. For this experiment, I have prepared five different concentrations of PO_4^{3-}. In Fig 3.15, the consumption of H_2S in controls was about 1mM, a decrease attributed to chemical oxidation. In the olivine samples after 4 hours of incubation, the [H_2S] reached similar values irrespective of the phosphate concentration. However, after 6 hours of incubation the [H_2S] was 0mM when phosphate was present, but higher in the absence of phosphate. My interpretation was that phosphate did not influence the rate but only the equilibrium of the reaction between H_2S and olivine. PO_4^{3-}, which is a weak iron chelator (Fe^{2+} and Fe^{3+}), is proposed to increase the solubility of olivine iron, making it more available for reaction with H_2S.

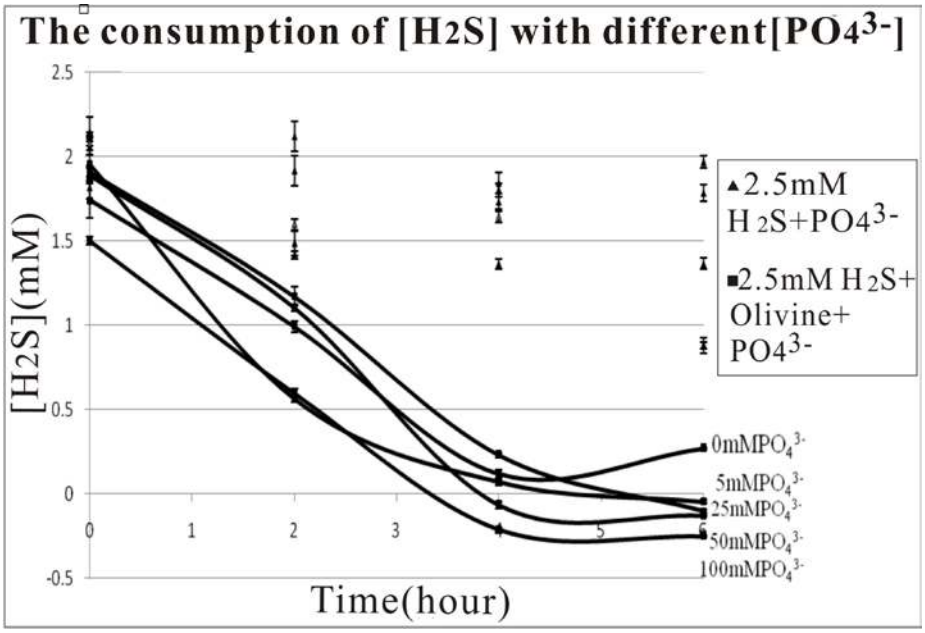

Fig 3.15. The evolution of [H_2S] during the reaction with olivine in the absence of olivine and with various concentrations of PO_4^{3-}. The error bars are standard deviations based on six replicate measurements of each sample and control.

The effect of olivine on the growth of DSR communities

To study the effect of olivine on the growth of DSR communities, we have analyzed growth at room temperature with stirring at 150 rpm. Our expectation was to find higher cell densities when olivine was present than with olivine present. One example of results showing the effect of olivine on the growth of a DSR community is shown in Fig. 3.16.

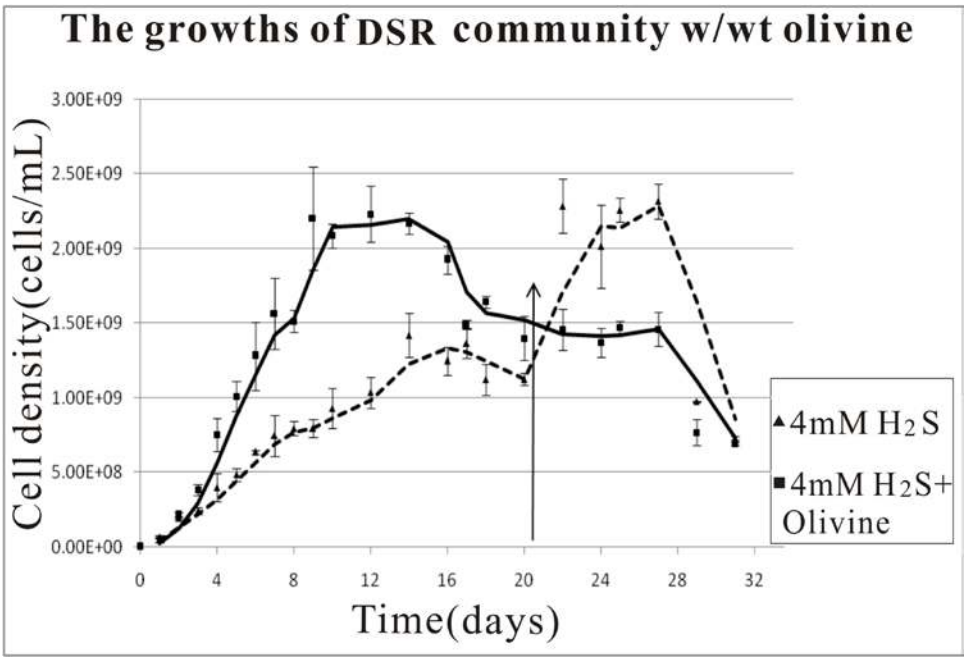

Fig 3.16. The growth of a DSR community in the presence and absence of olivine. The arrow indicates the day 20 when nutrients were added again to the incubation bottles. This was done because of the assumption that growth has slowed down, not because of lack of energy, but because of lack of nutrients. The error bars represent standard deviations based on five cell counting of each culture bottle.

In Fig. 3.16, the solid line represents the evolution of cell density in a sample containing olivine present in bottles, while the dash line represents a control without olivine. All cultures started from ~10^6 cells mL^{-1} and were incubated in 140mL sealed serum bottles containing 50mL of culture medium. Our results showed that when olivine was present the growth rate was faster during the exponential. The exponential phase was shorter (about 10 days) when olivine was present compared to controls without olivine (about 16 days). At the end of the exponential phase the cell density was very similar in samples (~2.1×10^9 cells/mL) and controls (~1.3×10^9 cells/mL). The inhibition

of growth in the stationary phase could have been due to accumulation of H2S or depletion of nutrients.

The nutrients added during day 20 contained organic acids and sulfate to a final concentration of 4mM $(NH_4)_2SO_4$, 10mM pyruvate, 20mM succinate, 20mM lactate and 10mM acetate. After the 20 day injection, the profile of the olivine sample did not change, cell density remained at a level of about $1.5x10^9$ cells/mL for eight more days after which (day 27) the death phase has begun. On the opposite, cells in control bottles proliferated and continued the exponential growth, peaking at 2.3 $x10^9$ cells/mL. Eventually growth stopped, the stationary phase was very brief and the control culture entered in the death phase in day 27. This rapid death is consisted with inhibition due to H_2S produced by dissimilatory sulfate reduction. This fast inhibition did not occurred in controls, most likely due to the reaction between H_2S and olivine.

Our results confirmed that the activity of DSR is positively influenced by the presence and abundance of olivine. DSRs ran out of nutrients faster when olivine was present and the final cell density was similar with and without olivine. This indicates that olivine is not as source of energy for DSR but most likely only a trap for H_2S. We hypothesize that olivine helps DSR obtain energy more efficiently.

Identify DSRs

To identify species present in our DSR communities, we have inoculated cultures in DSR roll tubes, and isolated colonies on LB plates in oxygen-free atmosphere. The approximate growth time between incubation and visible colonies was about 10 days at

room temperature. The clones we have isolated were putatively DSRs and facultative organotrophs. Two colony types were identified in the cultures. The general appearance of the colonies is shown Fig 3.17 A. The colonies were similar but were of different sizes.

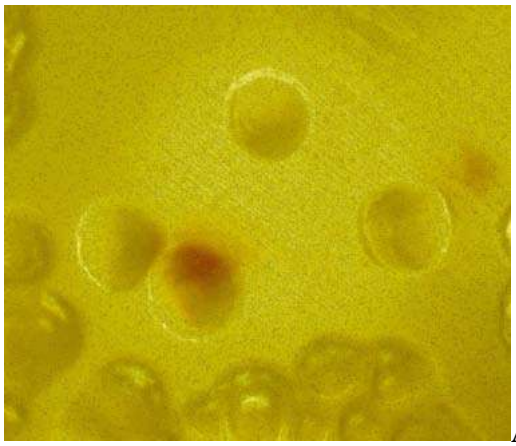
A
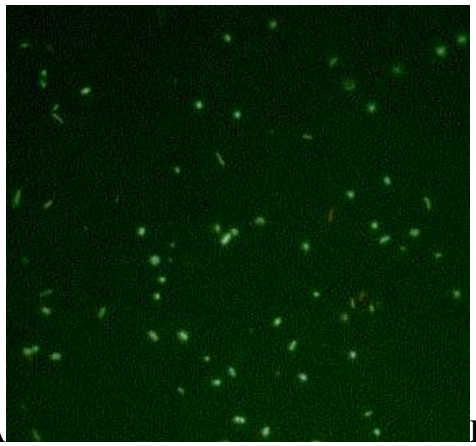
B

Fig 3.17. A: The appearance of DSR colonies on a LB plate (200X magnification using bright field microscopy). B: Acridine orange stained cells visualized in a DSR community grown in DSR medium without olivine (1000X magnification, epifluorescent microscopy).

Acridine orange stain (AO) is a differential stain for double vs single stranded nucleic acids. Double-stranded DNA has green fluorescence (around 520 nm) while single stranded DNA or RNA have an orange fluorescence (around 610 nm). Dead cells which contain fragments of single stranded DNA fluoresce orange (Darzynkiewicz et al., 1992) similar to cells showing high mRNA and rRNA expression. Resting cells (such as cells in stationary phase) fluoresce green. In Fig 3.17. image B, most cells had a green fluorescence.

We have attempted to extract DNA from DSR medium with olivine but although the concentration of DNA was high the PCR amplification was very poor. This was most likely due to increased concentration of iron. Attempts to clean the DNA samples were unsuccessful. Another concern was that the organotrophic isolates may not be DSR as well. In order to verify that our isolates were both organotrophic and DSR we have inoculated clones from each colony type in two types of culture media: a) 5% yeast extract with 10 mM lactate, 10 mM acetate, 10 mM succinate and 10 mM pyruvate (LASP); and b) DSR medium with LASP and olivine. If the olivine bottle has shown black precipitates, then the isolate was confirmed as positive for DSR activity and the yeast extract/LASP medium was used to separate biomass for DNA extraction. Both colony types separated from the role tubes were confirmed to be DSRs. We concluded that most isolates from the roll tubes and from the DSR community were dissimilatory sulfate reducers. Results have indicated that most DSR from the community we have worked with belong to two genera: *Pseudomonas* and *Clostridium/Desulfotomaculum*. *Pseudomonas* is a well known group of organotrophs with some sulfur oxidizing representatives. The strains of *Clostridium* we have isolated have close relatives that are DSRs (Fig 3.1.). Most likely these taxa are not the only DSRs in the community, but based on our results we believe these two genera were common in the DSR community we have used to analyze the effect of olivine on DSR.

Conclusions

My results showed that the reaction between H_2S produced by DSRs and olivine is abiotic, not catalyzed and exergonic. The pH does not vary during this process and changes in pH in the 5-9 range do not significantly influence this reaction. Bicarbonate inhibits the reaction between H_2S and olivine, but does not influence its equilibrium. Phosphate, which is a weak iron chelator, may increase the solubility of iron from olivine, and influence the equilibrium of the reaction and most likely the rate of olivine weathering in the presence of DSRs. The activity of DSRs is positively influenced by the presence and abundance of olivine. Olivine helps DSR obtaining energy more efficiently from DSR activity but it is unlikely to represent a source of energy or nutrients for the cells.

Based on our results we propose a potential mechanism to explain how DSR communities use olivine and grow on olivine surfaces. *Clostridium* utilizes organic acids (e.g. LASP) to reduce sulfate and produce hydrogen sulfide. Hydrogen sulfide is toxic to the cells but reacts with iron present on olivine surfaces leading to black iron sulfide precipitates. This reaction rate is controlled by the concentration of hydrogen sulfide when sufficient olivine was present, and it is not catalyzed or induced by bacteria activity. The fast reaction between hydrogen sulfide and olivine means that of the sulfide produced by *Clostridium* will begin reacting with olivine as soon after it is produced. Even if the full reaction may take hours to complete the concentration of hydrogen sulfide is kept low protecting the cells from its toxicity. The consumption of hydrogen

sulfide makes cells grow faster but, in my opinion, this is not due to the redox energy being added to the growth medium. Most of the iron sulfide formed in the reaction between hydrogen sulfide and olivine is amorphous FeS. This is important because unlike all other iron sulfides amorphous FeS is the only form that is easily oxidized with diosygen at room temperature. Our results indicated almost full oxidation of the amorphous FeS if the precipitates were exposed to air for 24 hours. I propose that in nature, some of the iron sulfides formed by DSR on olivine surfaces are chemically oxidized generating iron oxides and elemental sulfur. These chemicals are a byproduct of the corrosion of olivine induced by DSR, may help convert amorphous FeS into pyrite (FeS2) and can be used subsequently as oxidants on other processes such as iron reduction and sulfur oxidation. Both neutrophilic iron oxidation and sulfur reduction were cited among pseudomonads. Our results indicate that DSR communities are more complex than previously thought. The details of this mechanism and the diversity of olivine hosted DSR communities remains unknown.

Further research will have to include two parts. 1st. Study in more detail the mechanisms present in olivine hosted DSR communities, in particular the role associated microorganisms such as iron reducers and iron oxidizers. The formation of pyrite is important because pyrite is very stable and can be used as a biosignature of this activity. 2nd. Characterize the precipitates formed on olivine surfaces. More needs to be known about the evolution of the various mineral phases and amorphous precipitates from this process to describe its evolution.

References

Abreu F., Silva K.T., Martins J.L., Lins U.(2006) Cell viability in magnetotactic multicellular prokarayotes. *Int Microbiol* 9:267-272.

Abreu F., Silva K.T., Farina M., Keim C.N., Lins U.(2008) Greigite magenetosome membrane ultrastructure in *Candidatus* Magnetoglobus multicellularis. *Int Microbiol* 11:75-80.

Alt D. and Hyndman D. (1995) *Northwest Exposures: a Geologic Story of the Northwest*, Mountain Press Publishing Company, ISBN 0-87842-323-0.

Bahr M. et al.(2005) Molecular chacterization of sulfate reducing bacteria in a New England salt marsh. *Environ. Microbiol*. 7, 1175–1185.

Baker G. C., Smith J. J., Cowan D. A. (2003) Review and re-analysis of domain-specific 16S primers*, J. Microbiol. Meth.*, 55(3):541-555.

Barton L. L. and Fauque G.D.(2009). Biochemistry, physiology and biotechnology of sulfate-reducing bacteria. *Advances in Applied Microbiology* **58**: 41–98.

Bazylinski D.A., Frankel R.B., Jannasch H.W.(1988) Anaerobic magnetite production by a marine, magnetotactic bacterium, *Nature* 334:518-519.

Bazylinski D.A., Moskowitz B.M. (1997) Microbial biomineralization of magnetic iron minerals: Microbiology, magnetism and environmental significance. *Rev Mineral* 35:181-223.

Bazylinski D.A., Frankel R.B. (2003) Biologically controlled mineralization in prokaryotes. In: Dove PM, De Yoreo JJ, Weiner S (eds)

Biomineralization, Reviews in Mineralogy and Geochemistry, Vol. 54. *Min Soc Amer Geochem Soc* pp 217-247.

Bazylinski D.A., Frankel R.B.(2004) Magnetosome formation in prokaryotes. *Nature Rev Microbiol* 2:217-230.

Ben-Dov E., Brenner A. and Kushmaro A.(2007) Quantification of sulfate-reducing bacteria in industrial wastewater by real-time polymerase chain reaction (PCR) using dsrA and apsA genes. *Microb. Ecol*. 54, 439–451.

Bertani L.E., Huang J.S., Weir B.A., Kirschvink J.L. (1997) Evidence for two types of subunits in the bacterioferritin of *Magnetospirillum magnetotacticum*. *Gene* 201:31-36

Blakemore R.P.(1975) Magnetotactic bacteria. *Science* 190:377-379.

Blakemore R.P.(1982) Magnetotactic bacteria. *Annu Rev Microbiol* 36:217-38.

Blakemore R.P., Short R.A., Bazylinski C., Rosenblatt C., Frankel R.B. (1985) Microaerobic conditions are required for magnetite formation within *Aquaspirillum magnetotacticum*. *Geomicrobiol J* 4:53-71

Campbell L.L., Postgate J.R.(1965) Classification of the spore-forming sulfate-reducing bacteria. *Bacteriol Rev.* 29(3):359–363.

Chang I.S., Shin P.K. and Kim B.H. (2000) Biological treatment of acid mine drainage under sulfate-reducing conditions with solid waste materials as substrate. *Wat Res*, 34:1269-1277.

Colleran E., Finnegan S., Lens P.(1995) Anaerobic treatment of sulphate-containing

waste streams, *Anton. Leeuw*. 67 (1) 29–46.
Cox B.L., Popa R., Bazylinski D.A., Lanoil B., Douglas S., Belz A., Engler D.L., Nealson K.H. (2002) Organization and elemental analysis of P-, S-, and Fe-rich inclusions in a population of freshwater magnetococci*, Geomicrobiol J* 19:387-406.
Csákberényi-Malasicsa D., Rodriguez-Blanco J.D. et al. (2012) Structural properties and transformations of precipitated FeS *Chemical Geology* 294-295, 249-258.
Darzynkiewicz Z., Bruno S., Del Bino G., Gorczyca W., Hotz M.A., Lassota P., Traganos F. (1992) Features of the apoptotic cells measured by flow cytometry. *Cytometry* 13, 795-808.
de Bruijn F.J. (1992) Use of repetitive (repetitive extragenic palindromic and enterobacterial repetitive intergenic consensus) sequences and the polymerase chain reaction to fingerprint the genomes of *Rhizobium meliloti* isolates and other soil bacteria. *Appl. Environ. Microbiol.* 58: 2180-2187.
Dubilier N. et al.(2001) Endosymbiontic sulphate-reducing and sulphide-oxidizing bacteria in an oligochaete worm. *Nature* 411, 298–302.
Elliott P., Ragusa S.and Catcheside D. (1998). Growth of sulfate reducing bacteria under acidic conditions in an anaerobic bioreactor as a treatment system for acid mine drainage. *Wat Res*, 32: 3724-3730.
Emerson D. and Moyer C. L.(1997) Isolation and characterization of novel iron-oxidizing bacteria that grow at circumneutral pH. *Appl. Environ. Microbiol*. 63:4784-4792.
Fortin D., Ferris F.G., Beveridge T.J.(1997) Surface-mediated mineral development by bacteria. *Rev Mineral* 35:161-180.
Frankel R.B.(1981) Bacterial magnetotaxis vs. geotaxis. *Trans Am Geophys Soc* (EOS) 62:850.
Frankel R.B., Papaefthymiou G.G., Blakemore R.P., O'Brien W.(1983) Fe_3O_4 precipitation in magnetotactic bacteria. *Biochim Biophys Acta* 763:147-159.
Frankel R.B., Papaefthymiou G.C., Blakemore R.P.(1985) Mössbauer spectroscopy of iron biomineralization products in magnetotactic bacteria. In: Kirschvink J.L., Jones D.S., MacFadden B.J. (eds) Magnetite biomineralization and magnetoreception in organisms. *Plenum*, New York, pp 269-287.
Frankel R.B.(1990) Iron biominerals: an overview. In: Frankel R.B., Blakemore R.P. (eds) *Iron biominerals.* Plenum, New York, 1–6.
Frankel R.B., Bazylinski D.A., Johnson M.S., Taylor B.L.(1997) Magnetoaerotaxis in marine coccoid bacteria*. Biophys* J 73:994-1000.
Frankel R.B., Bazylinski D.A., Schuler D. (1998) Biomineralization of magnetic iron minerals in magnetotactic bacteria. *Supramol Sci* 5: 383-390.
Frederick M.M., Antao S.M. et al.(2005) Resolving Structure and Size of Amorphous Mineral Precipitates by PDF Analysis. *Acta Cryst.* A61, C377
Garcia B., Lemelle L., Rose-Koga E. F. et al (2005) The Mg-isotope biosignature of *Escherichia coli*-mediated olivine dissolution, *American Geophysical Union*, Fall Meeting 2005, abstract #PP34A-03.
Geets J. et al. (2006) DsrB gene-based DGGE for community and diversity surveys of

sulphate-reducing bacteria. *J. Microbiol. Methods* 66, 194–205.
Gorby Y.A., Beveridge T.J., Blakemore R.P.(1988) Characterization of the bacterial magnetosome membrane. *J Bacteriol* 170:834-841.
Greenberg A.E., Trussell R.R., Clesceri L.S. (eds) (1985) Standard methods for the examination of water and wastewater, 16th ed. APHA-AWWAWPCF. Port City Press, Baltimore.
Grunberg K., Wawer C., Tebo B.M., Schuler D. (2001) A large gene cluster encoding several magnetosome proteins is conserved in different species of magnetotactic bacteria. *Appl Environ Microbiol* 67:4573-4582.
Guenther E., Johnson K.S. and Coale K.H.(2001) Direct utraviolet spectrophotometric determination of total sulfide and iodide in natural waters. *Anal. Chem*. 2001, 73, 3481-3487.
Harmandas N.G., Koutsoukos P.G. (1996) The formation of iron (II) sulfides in aqueous environments. *Journal of Crystal Growth* 167, 719-724.
Hem J.D.(1960) Restraints on dissolved ferrous iron imposed by bicarbonate redox potential, and pH from *Chemistry of iron in natural water*. Geological survey water supply paper, 1459-B
Heyen U., Schüler D. (2003) Growth and magnetosome formation by microaerophilic *Magnetospirillum* strains in an oxygen-controlled fermentor. *Appl Microbiol Biotechnol* 61:536-544.
Hines M. E. et al.(1999) Molecular phylogenetic and biogeochemical studies of sulfate-reducing bacteria in the rhizosphere of *Spartina alterniflora*. *Appl. Environ. Microbiol.* 65, 2209–2216.
Itoh T., Suzuki K-I. and Nakase T. (1998) *Thermocladium* modestius gen. nov., sp. nov. a new genus of rodshaped, extremely thermophilic crenarchaeote. *Int. J. Syst. Bacteriol.* 48, 879–887.
Itoh T., Suzuki K-I., Sanches P. C. and Nakase T. (1999)*Caldivirga maquilingensis* gen. nov., sp. nov. a new genus of rod-shaped crenarchaeote isolated from a hot spring in the Philippines. *Int. J. Syst. Bacteriol*. 49, 1157–1163.
Ivanov M.V.(1981) The global biogeochemical sulphur cycle, In Likens G.E. (Eds.) *Some Perspectives of the Major Biogeochemical Cycle*, Scope, 61-78.
Janssen A. J. H., Ruitenberg R. and Buisman C. J. N.(2001) Industrial applications of new sulphur biotechnology. *Water Sci. Technol*. 44, 85–90.
Jeanthon C. et al. (2002) *Thermodesulfobacterium hydrogeniphilum* sp. nov., a thermophilic, chemolithoautotrophic sulfate-reducing bacterium isolated from a deep-sea hydrothermal vent at Guaymas Basin and emendation of the genus *Thermodesulfobacterium*. *Int. J. Syst. Evol. Microbiol.* 52, 765–772.
Jones H.E., Trudinger P.A., Chambers L.A. and Pyliotis N.A.(1976) Metal accumulation by bacteria with particular reference to dissimilatory sulphate-reducing bacteria. *Z.Allg. Mikrobiol*. 16: 425-435.
Jong T. and Parry D.L.(2003) Removal of sulfate and heavy metals by sulfate reducing bacteria in short-term bench scale upflow anaerobic packed bed reactor runs. *Wat Res*, 37: 3379–3389.

Josef, J. A., M. R. Fisk, and S. Giovannoni (2007) Peridotite dissolution rates in microbial enrichment cultures. In Kelemen, P.B., E. Kikawa, and D. J. Miller (Eds.), *Proc. ODP, Sci. Results*, 209: College Station, TX (Ocean Drilling Program), 1–38.

Kawaguchi R., Burgess J.G., Sakaguchi T., Takeyama H., Thornhill R.H., Matsunaga T. (1995) Phylogentic analysis of a novel sulfate-reducing magnetic bacterium, RS-1, demonstrates its membership of the Proteobacteria. *FEMS Microbiol Lett* 126:277-282.

Keim C.N., Solórzano G., Farina M., Lins U.(2005) Intracellular inclusions of uncultured magnetotactic bacteria. *Int Microbiol* 8:111-117.

Kim S.D., Kilbane J.J. and Cha D.K. (1999) Prevention of acid mine drainage by sulfate reducing bacteria: organic substrate addition to mine waste piles. *Env Eng Sci*, 16: 139-45

Kirschvink J.L.(1980) South-seeking magnetic bacteria. *J Exp Biol* 86:345-347.

Kirschvink J.L. (1982) Birds, bees and magnetism: A new look at the old problem of magnetoreception. *Trends Neuroscien* 5:160-167.

Kirschvink J.L., Jones D.S., MacFadden B.J. (eds) (1985): *Magnetite biomineralization and magnctoreception in organisms: A new biomagnetism.* New York: Plenum Press. 682 pp.

Klenk et al. (1997) The complete genome sequence of the hyperthermophilic, sulphate-reducing archaeon *Archaeoglobus fulgidus* Nature 390, 364-370.

Kliushnikova T.M., Chernyshenko D.V., Kasatkina T.P.(1992) The sulfate-reducing capacity of bacteria in the genus *Pseudomonas. Mikrobiol Zh.*, 54(2), 49-54.

Knittel K. et al. (2003) Activity, distribution, and diversity of sulfate reducers and other bacteria in sediments above gas hydrate (Cascadia Margin, Oregon). *Geomicrobiol. J.* 20, 269–294.

Komeili A., Vali H., Beveridge T.J., Newman D.K. (2004) Magnetosome vesicles are present before magnetite formation, and MamA is required for their activation. *Proc Natl Acad Sci* USA 101:3839-3844.

Latimer W. M.(1952) *Oxidation potentials*. New York, Prentice-Hall, 392 pages.

Ledin M., Pedersen K.(1996) The environmental impact of mine wastes roles of microorganisms and their significance in treatment of mine wastes. *Earth-Sci Rev* 41: 67-108.

Longazo, T.G., Wentworth, S.J., McKay, D.S., Southam, G., and Clemett, S.J. (2001)
Olivine weathering: abiotic versus biotic processes as possible biosignatures. *Lunar Planet. Sci.*, 32:2013.

Lowenstam H.A.(1962) Magnetite in denticle capping in recent chitons (*polyplacophora*). *Geol Soc Am Bull*. 73:435--438.

Lowenstam H. A. and Weiner S.(1989) *On Biomineralization*, Oxford University Press, Oxford, 324 pages.

Lowry O.H., Rosebrough N.J., Farr A.L. and Randall R.J.(1951) Protein measurement with the Folin-Phenol reagents. *J Biol Chem* 193:265-275.

MacIntire W.H. and Marshall H.L.(1959). Magnesium ammonium phosphate from

olivine and rock phosphate. *Agric. Food Chem*. 7:566-568.
Madigan M.T., Martino J.M. (2006) *Brock Biology of Microorganisms* (11th ed.). Pearson. p.136.
Matsunaga T., Sakaguchi T., Tadokoro F. (1991) Magnetite formation by a magnetic bacterium capable of growing aerobically. *Appl Microbiol Biotechnol* 35:651-655.
Matsunaga T., Okamura Y. (2003) Genes and proteins involved in bacterial magnetic particle formation. *Trends Microbiol* 11:536-541.
Matsunaga T., Okamura Y., Tanaka T. (2004) Biotechnological application of nano-scale engineered bacterial magnetic particles. *J Mater Chem* 14:2099-2105.
Mattorano D. A. and Merinar T.(1999) Respiratory protection on offshore drilling rigs. *Appl. Occup. Environ. Hyg*. 14, 141–148..
Mazza G., Cascio P. and Barbieri E.(2003) Composti volatili liberi e glicoconiugati presenti nelle foglie e negli acini della *Vitis vinifera* Cv Moscato bianco. *Riv. Vitic. Enol.* 56, 57-74.
McConnaughey T. (1989) ^{13}C and ^{18}O isotopic disequilibrium in biological carbonates: I. Patterns. *Geochim Cosmochim Acta* 53:151-162.
McKinley J. P., Stevens T.O. (2000) Microfossils and paleoenvironments in deep subsurface basalt samples, *Geomicrobiology Journal*, 17:43-54.
Michel F.M., Antao S.M., Chupas P.J., Lee P.L, Parise J.B., Schoonen M.A.A.(2005) Short- to medium-range atomic order and crystallite size of the initial FeS precipitate from pair distribution function analysis. *Chem. Mater*., 17, 6246-6255.
Minz D. et al. (1999) Diversity of sulfate-reducing bacteria in oxic and anoxic regions of a microbial mat characterized by comparative analysis of dissimilatory sulfite reductase genes. *Appl. Environ. Microbiol.* 65, 4666–4671.
Mori K., Kim H., Kakegawa T. and Hanada S. (2003) A novel lineage of sulphate-reducing microorganisms: *Thermodesulfobiaceae* fam. nov., *Thermodesulfobium narugense*, gen. nov., sp. nov. a new thermophilic isolate from a hot spring. *Extremophiles* 7, 283–290.
Moskowitz B.M., Frankel R.B., Flanders P.J., Blakemore R.P., Schwartz B.B. (1988) Magnetic properties of magnetotactic bacteria. *J Magn Magn Mat* 73:273-288.
Moskowitz B.M., Frankel R.B., Bazylinski D.A.(1993) Rock magnetic criteria for the detection of biogenic magnetite. *Earth Planet Sci Lett* 120:283-300.
Mullet M., Boursiquot S., Ehrhardt J. (2004) *Colloids Surf. A* , 244, 77-85.
Mussmann M., Ishii K., Rabus R. and Amann R. (2005) Diversity and vertical distribution of cultured and uncultured *Deltaproteobacteria* in an intertidal mud flat of the Wadden Sea. *Environ. Microbiol.* 7, 405–418.
Muyzer G., and Stams A.J.M. (2008) The ecology and biotechnology of sulfate-reducing bacteria. *Nat Rev Microbiol* 6: 441–545.
Nakamura C.J., Burgess G., Sode K., Matsunaga T. (1995) An iron-regulated gene, *magA*, encoding an iron transport protein of *Magnetospirillum* sp. strain AMB-1. *J Biol Chem* 270:28392-28396.
Nilsen R. K., Beeder J.,Thostenson T. and Torsvik T. (1996) Distribution of thermophilic marine sulfate reducers in North Sea oil field waters and oil reservoirs. *Appl.*

Environ. Microbiol. 62, 1793–1798.
Okamura Y., Takeyama H., Matsunaga T.(2001) A magnetosome-specific GTPase from the magnetic bacterium *Magnetospirillum magneticum* AMB-1. *J Biol Chem* 276:48183-48188.
Oude Elferink S. J. W. H.,Visser A., Hulshoff-Pol L. W. and Stams A. J. M. (1994) Sulphate reduction in methanogenic bioreactors. *FEMS Microbiol. Rev.* 15, 119–136.
Paoletti L.C., Blakemore R.P. (1986) Hydroxamate production by *Aquaspirillum magnetotacticum*. *J Bacteriol* 167:73-76.
Popa R., Smith A.R. et al.(2012) Olivine-respiring bacteria isolated from the rock-ice interface in a lava-tube cave, a mars analog environment, *Astobiology*, Volume 12, Number 1,9-18.
Postgate J.R.(1984) *The Sulphate Reducing Bacteria*, (2nd ed), University Press, Cambridge.
Rabus R., Hansen T.A., Widdel F.(2006) Dissimilatory sulfate- and sulfur-reducing, in: Dworkin M., Falkow S., Rosenberg E., Schleifer K.H., Stackebrandt E.(Eds.), *The Prokaryotes*,(3rd ed) vol. 2, Springer, New York, 659–768.
Reis M.A.M., Almeida J.S., Lemos P.C., Carrondo M.J.T.(1992) Effect of hydrogen sulfide on growth of sulfate reducing bacteria. *Biotechnology and Bioengineering* 40, Issue 5, pages 593–600.
Rickard D. and Luther G.W.(2007) Chemistry of iron sulfides. *Chem.Rev.*107, 514-562.
Rissati J. B., Capman W. C. and Stahl D. (1994) A. Community structure of a microbial mat: the phylogenetic dimension. *Proc. Natl Acad. Sci. USA* 91, 10173–10177.
Robertson L.A., Kuenen J.G.(2006) The colorless sulphur bacteria, in: Dworkin M., Falkow S., Rosenberg E., Schleifer K.H., Stackebrandt E. (Eds.), *The Prokaryotes*, (3rd ed) vol. 2, Springer, New York, 985–1011.
Sakaguchi T., Tsujimura N., Matsunaga T.(1996) A novel method for isolation of magnetic bacteria without magnetic collection using magnetotaxis. *J Microbiol Meth* 26:139-145.
Sass H., Wieringa E., Cypionka H., Babenzien H. D. and Overmann J. (1998) High genetic and physiological diversity of sulfate-reducing bacteria isolated from an oligotrophic lake sediment. *Arch. Microbiol*. 170, 243–251.
Scheffel A., Gruska M., Faivre D., Linaroudis A., Plitzko J.M., Schuler D. (2006) An acidic protein aligns magnetosomes along a filamentous structure in magnetotactic bacteria. *Nature* 440:110-114.
Schmidt W.J. (1924) Die bausteine des tierkorpers in polarisiertem lichte. *F. Cohen Verlag*, Bonn.
Schüler D., Uhl R., Baeuerlein E.(1995) A simple light scattering method to assay magnetism in *Magnetospirillum gryphiswaldense*. *FEMS Microbiol Lett* 132:139-145.
Schüler D., Baeuerlein E.(1997) Iron transport and magnetite crystal formation of the magnetic bacterium *Magnetospirillum gryphiswaldense. J Physiq* IV 7(C1):647-650.

Schüler D., Baeuerlein E.(1998) Dynamics of iron uptake and Fe_3O_4 biomineralization during aerobic and microaerobic growth of *Magnetospirillum gryphiswaldense. J Bacteriol* 180:159-162.

Schüler D., Frankel R.B. (1999) Bacterial magnetosomes: microbiology, biomineralization and biotechnological applications. *Appl Microb Biotech* 52:464-473.

Schüler D.(1999) Formation of magnetosomes in magnetotactic bacteria. *J Molec Microbiol Biotechnol* 1:79-86.

Schüler D. (2002) The biomineralization of magnetosomes in *Magnetospirillum gryephiswaldense. Int Microbiol* 5:209-214.

Schulz, H. D. and Zabel, M. (eds) (2000). *Marine Geochemistry*. Springer-Verlag.

Sen A.M.(2001) *Acidophilic Sulphate Reducing Bacteria: Candidates for Bioremediation of Acid Mine Drainage Pollution.* Thesis, Univ. Wales

Short K.A., Blakemore R.P.(1986) Iron respiration-driven proton translocation in aerobic-bacteria. *J Bacteriol* 167:729-731.

Siering P.L., and Ghiorse W.C.(1996) Phylogeny of the Sphaerotilus-Leptothrix group inferred from morphological comparisons, genomic fingerprinting, and 16S ribosomal DNA sequence analyses. *Int. J. Syst. Bacteriol*. 46: 173-182.

Siever R. and Woodford N.(1979) Dissolution kinetics and the weathering of mafic minerals. *Geochim. Cosmochim. Acta.* 43,717–724.

Sigel A., Sigel H. and Sigel R. K.O., ed. (2008). *Biomineralization: From nature to application*. Metal ions in life sciences. 4. Wiley.

Simkiss K. and Wilbur K. M.(1989) *Biomineralization*, Academic Press, N.Y., 337 pages.

Smirnov A.V., Tarduno J.A. (2002) Magnetic field control of the low-temperature magnetic properties of stoichiometric and cation-deficient magnetite. *Earth Planet Sci Lett* 194:359-368.

Spring S., Amann R., Ludwig W., Schleifer K.H., van Gemerden H., Petersen N. (1993) Dominating role of an unusual magnetotactic bacterium in the microaerobic zone of a freshwater sediment. *Appl Env Microbiol* 59:2397-2403.

Spring S., Schleifer K.H. (1995) Diversity of magnetotactic bacteria*. System Appl Microbiol* 18:147-153.

Stadnitskaia A. et al.(2005) Biomarker and 16S rDNA evidence for anaerobic oxidation of methane and related carbonate precipitation in deep-sea mud volcanoes of the Sorokin Trough, Black Sea. *Mar. Geol*. 217, 67–96.

Stefan M.S., Ronald P. K., and Heide N. S.(2007) The sulfur cycle *Oceanography*, Volume 20, Number 2, 117-124.

Steinberger B., Petersen N., Petermann H., Weiss D.G. (1994) Movement of magnetic bacteria in time-varying magnetic-fields. *J Fluid Mech* 273:189-211.

Tang K., Baskaran V., Nemati M. (2009) Bacteria of the sulphur cycle: An overview of microbiology, biokinetics and their role in petroleum and mining industries. *Biochemical Engineering Journal* 44, 73–94.

Thomas C.M.(ed) (1998) *Biotechnology Handbooks 10, Pseudomonas* Plenum Press,

New York and London. ISBN 0-306-45849-7, 335pages.
Thomas-Keprta K.L., Clemett S.J., Bazylinski D.A., et al. (2001) Truncated hexa-octahedral magnetite crystals in ALH84001: Presumptive biosignatures. *Proc Natl Acad Sci* USA 98:2164-2169.
Trudinger P.A., Lambert I.B., and Skyring G.W.(1972) Biogenic sulfide ores: A feasibility study. *Econ. Ceol.* 67: 1114-1127.
Tsakraklides G., Martin M., Chalam R., Tarczynski M.C., Schmidt A. and Leustek T. (2002) Sulfate reduction is increased in transgenic Arabidopsis thaliana expressing 5'-adenylylsulfate reductase from *Pseudomonas aeruginosa*. *Plant J.* 32: 879-889.
Vainshtein M.B., Suzina N.E., Kudryashova E.B., Ariskina E.V., Sorokin V.V. (1998) On the diversity of magnetotactic bacteria. *Microbiologiya* 67:670-676.
Vaughan D. J.; Craig J. R.(1978) *Mineral Chemistry of Metal Sulfides*. Cambridge University Press: New York
Walker M.M., Kirschvink J.L., Chang S-B. R., Dizon A.E.(1984) A candidate magnetic sense organ in the yellowfin tuna *Thunnus albacares*. *Science* 224:751-753.
Webster G. et al.(2006) A comparison of stable isotope probing of DNA and phospholipids fatty acids to study prokaryotic functional diversity in sulfate-reducing marine sediment enrichment slurries. *Environ. Microbiol*. 8, 1575–1589.
Weiner S., Dove P.M.(2003) An overview of biomineralization processes and the problem of the vital effect. *Mineralogy and Geochemistry*, Vol. 54, No. 1, 1-29.
Welch S.A., and Banfield J.F.(2002) Modification of olivine surface morphology and reactivity by microbial activity during chemical weathering. *Geochimica et Cosmochimica Acta* 66:213-221.
White A.F., and Yee A. (1985) Aqueous oxidation-reduction kinetics associated with coupled electron-cation transfer from iron containing silicates at 25°C. *Geochim. Cosmochim. Acta.* 49, 1263–1275.
Wogelius R. A. and Walther J. V.(1992) Olivine dissolution kinetics at near surface conditions. *Chem. Geol*. 97, 101–112.
Wolthers M., Van der Gaast S. J., Rickard D. (2003) The structure of disordered mackinawite. *American Mineralogist* 88, 2007-2015.
Woyke T. et al.(2006) Symbiosis insights through metagenomic analysis of a microbial consortium. *Nature* 443, 950–955.